

# When One Level Is Not Enough

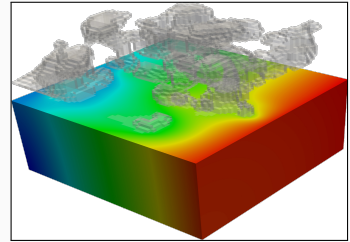
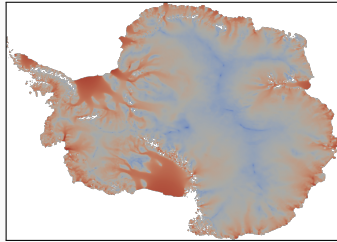
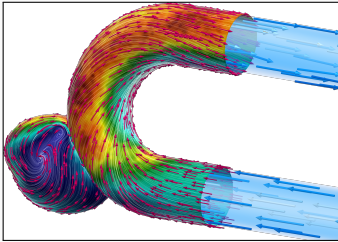
Multilevel Domain Decomposition Methods for Physics and Data-Driven Problems

---

Alexander Heinlein<sup>1</sup>

Scientific Computing Seminar, IWR, Heidelberg University, Germany, December 5, 2024

<sup>1</sup>Delft University of Technology



## Numerical methods

### Based on physical models

- + Robust and generalizable
- Require availability of mathematical models

## Machine learning models

### Driven by data

- + Do not require mathematical models
- Sensitive to data, limited extrapolation capabilities

## Scientific machine learning (SciML)

Combining the strengths and compensating the weaknesses of the individual approaches:

numerical methods **improve** machine learning techniques  
machine learning techniques **assist** numerical methods

## 1 Classical Schwarz Domain Decomposition Methods

## 2 Schwarz Domain Decomposition Preconditioners

Based on joint work with

**Axel Klawonn** and **Jascha Knepper**

(University of Cologne)

**Mauro Perego** and **Siva Rajamanickam**

(Sandia National Laboratories)

**Oliver Rheinbach** and **Friederik Röver**

(TU Bergakademie Freiberg)

**Kathrin Smetana**

(Stevens Institute of Technology)

**Olof Widlund**

(New York University)

## 3 Domain Decomposition for Neural Networks

Based on joint work with

**Eric Cyr**

(Sandia National Laboratories)

**Victorita Dolean**

(Eindhoven University of Technology)

**Siddhartha Mishra**

(ETH Zürich)

**Ben Moseley**

(Imperial College London)

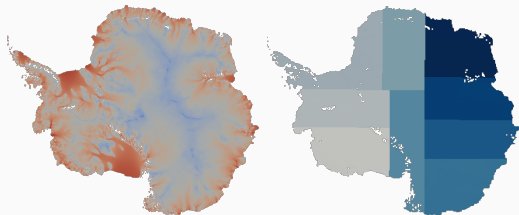
**Corné Verburg**

(Delft University of Technology)

# Classical Schwarz Domain Decomposition Methods

---

# Domain Decomposition Methods



Images based on [Heinlein, Perego, Rajamanickam \(2022\)](#)

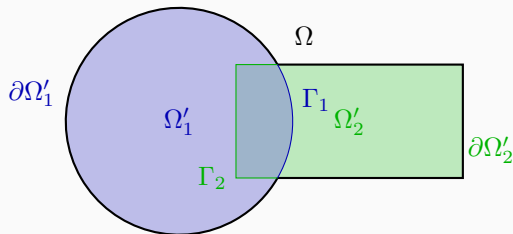
**Historical remarks:** The **alternating Schwarz method** is the earliest **domain decomposition method (DDM)**, which has been invented by **H. A. Schwarz** and published in **1870**:

- Schwarz used the algorithm to establish the **existence of harmonic functions** with prescribed boundary values on **regions with non-smooth boundaries**.

## Idea

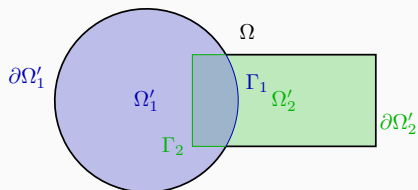
Decomposing a large **global problem** into smaller **local problems**:

- **Better robustness** and **scalability** of numerical solvers
- **Improved computational efficiency**
- Introduce **parallelism**



# The Alternating Schwarz Algorithm

For the sake of simplicity, instead of the two-dimensional geometry,



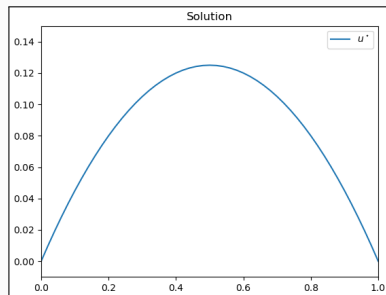
we consider the **one-dimensional Poisson equation**

$$\begin{aligned} -u'' &= 1 \quad \text{in } [0, 1], \\ u(0) &= u(1) = 0. \end{aligned}$$

**Overlapping domain decomposition:**



**Solution:**  $u(x) = -\frac{1}{2}x(x-1).$



Let us consider the simple boundary value problem: Find  $u$  such that

$$-u'' = 1, \text{ in } [0, 1], \quad u(0) = u(1) = 0$$

We perform an **alternating Schwarz iteration**:

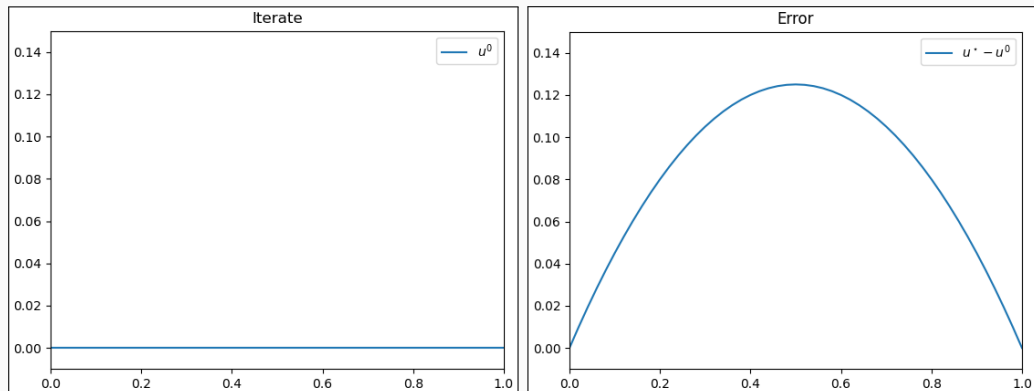


**Figure 1:** Iterate (left) and error (right) in iteration 0.

Let us consider the simple boundary value problem: Find  $u$  such that

$$-u'' = 1, \text{ in } [0, 1], \quad u(0) = u(1) = 0$$

We perform an **alternating Schwarz iteration**:

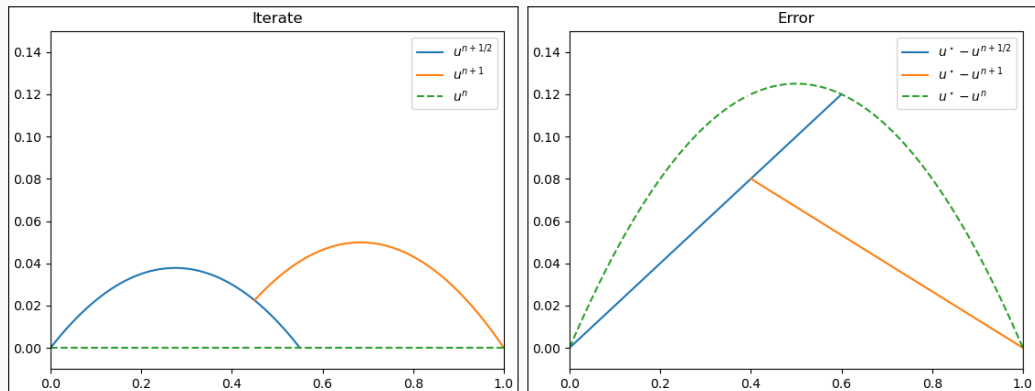


**Figure 1:** Iterate (left) and error (right) in iteration 1.



Let us consider the simple boundary value problem: Find  $u$  such that

$$-u'' = 1, \text{ in } [0, 1], \quad u(0) = u(1) = 0$$

We perform an **alternating Schwarz iteration**:

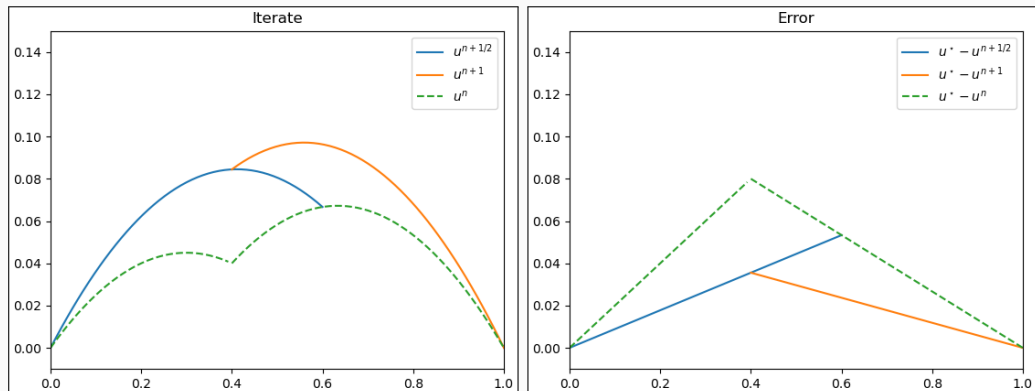


**Figure 1:** Iterate (left) and error (right) in iteration 2.

Let us consider the simple boundary value problem: Find  $u$  such that

$$-u'' = 1, \text{ in } [0, 1], \quad u(0) = u(1) = 0$$

We perform an **alternating Schwarz iteration**:

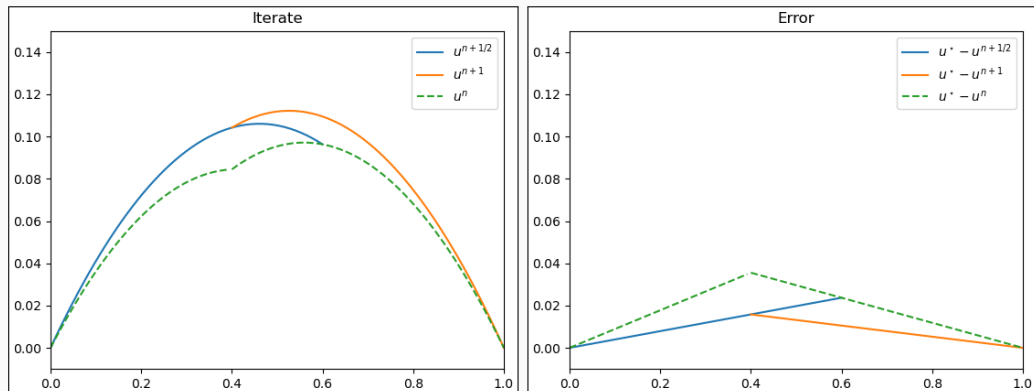


**Figure 1:** Iterate (left) and error (right) in iteration 3.

Let us consider the simple boundary value problem: Find  $u$  such that

$$-u'' = 1, \text{ in } [0, 1], \quad u(0) = u(1) = 0$$

We perform an **alternating Schwarz iteration**:

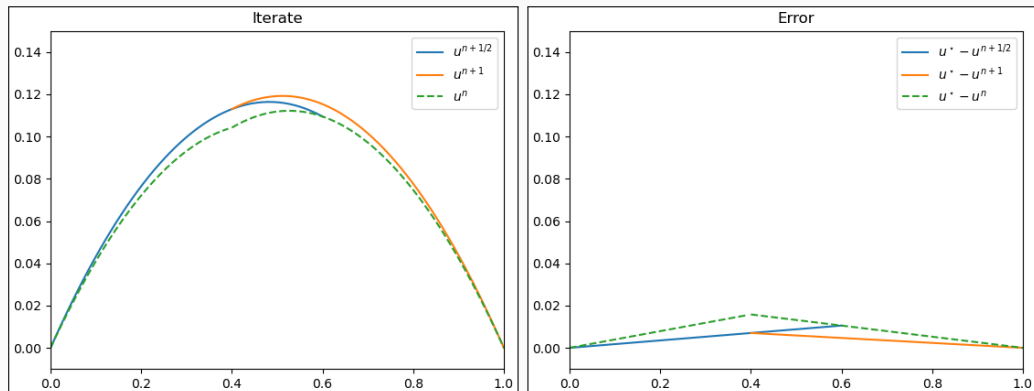


**Figure 1:** Iterate (left) and error (right) in iteration 4.

Let us consider the simple boundary value problem: Find  $u$  such that

$$-u'' = 1, \text{ in } [0, 1], \quad u(0) = u(1) = 0$$

We perform an **alternating Schwarz iteration**:

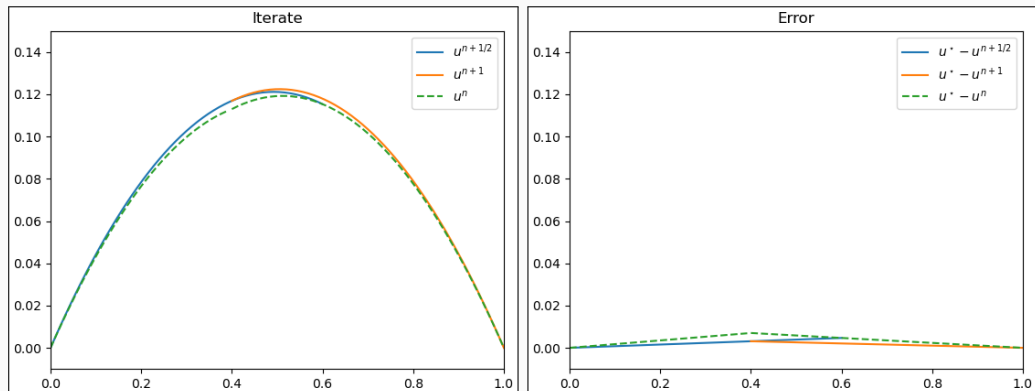


**Figure 1:** Iterate (left) and error (right) in iteration 5.

The alternating Schwarz algorithm is **sequential** because **each local boundary value problem** depends on the solution of the **previous Dirichlet problem**:

$$(D_1) \begin{cases} -\Delta u^{n+1/2} = f & \text{in } \Omega'_1, \\ u^{n+1/2} = \mathbf{u}^n & \text{on } \partial\Omega'_1 \\ u^{n+1/2} = \mathbf{u}^n & \text{on } \Omega \setminus \overline{\Omega'_1} \end{cases}$$
$$(D_2) \begin{cases} -\Delta u^{n+1} = f & \text{in } \Omega_2, \\ u^{n+1} = \mathbf{u}^{n+1/2} & \text{on } \partial\Omega'_2 \\ u^{n+1} = \mathbf{u}^{n+1/2} & \text{on } \Omega \setminus \overline{\Omega'_2} \end{cases}$$



**Idea:** For all red terms, we use the values from the previous iteration. Then, the both Dirichlet problem can be solved at the same time.

The alternating Schwarz algorithm is **sequential** because **each local boundary value problem** depends on the solution of the **previous Dirichlet problem**:

$$(D_1) \begin{cases} -\Delta u^{n+1/2} = f & \text{in } \Omega'_1, \\ u^{n+1/2} = \mathbf{u}^n & \text{on } \partial\Omega'_1 \\ u^{n+1/2} = \mathbf{u}^n & \text{on } \Omega \setminus \overline{\Omega'_1} \end{cases}$$
$$(D_2) \begin{cases} -\Delta u^{n+1} = f & \text{in } \Omega_2, \\ u^{n+1} = \mathbf{u}^{n+1/2} & \text{on } \partial\Omega'_2 \\ u^{n+1} = \mathbf{u}^{n+1/2} & \text{on } \Omega \setminus \overline{\Omega'_2} \end{cases}$$



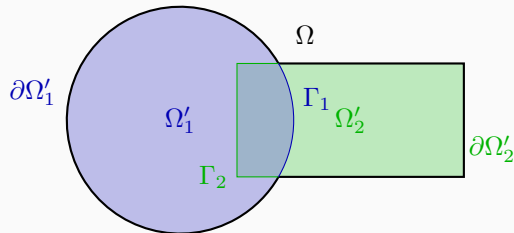
**Idea:** For all red terms, we **use the values from the previous iteration**. Then, the both Dirichlet problem **can be solved at the same time**.

# The Parallel Schwarz Algorithm

The **parallel Schwarz algorithm** has been introduced by **Lions (1988)**. Here, we solve the local problems

$$(D_1) \begin{cases} -\Delta u_1^{n+1} = f & \text{in } \Omega'_1, \\ u_1^{n+1} = u_2^n & \text{on } \partial\Omega'_1, \end{cases}$$

$$(D_2) \begin{cases} -\Delta u_2^{n+1} = f & \text{in } \Omega_2, \\ u_2^{n+1} = u_1^n & \text{on } \partial\Omega'_2. \end{cases}$$



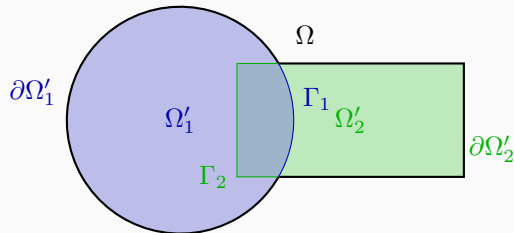
Since  $u_1^n$  and  $u_2^n$  are both computed in the previous iteration, the problems can be solved independent of each other.

# The Parallel Schwarz Algorithm

The **parallel Schwarz algorithm** has been introduced by **Lions (1988)**. Here, we solve the local problems

$$(D_1) \begin{cases} -\Delta u_1^{n+1} = f & \text{in } \Omega'_1, \\ u_1^{n+1} = u_2^n & \text{on } \partial\Omega'_1, \end{cases}$$

$$(D_2) \begin{cases} -\Delta u_2^{n+1} = f & \text{in } \Omega_2, \\ u_2^{n+1} = u_1^n & \text{on } \partial\Omega'_2. \end{cases}$$



Since  $u_1^n$  and  $u_2^n$  are both computed in the previous iteration, the problems can be solved independent of each other.

This method is suitable for **parallel computing!**





Let us again consider the simple boundary value problem: Find  $u$  such that

$$-u'' = 1, \text{ in } [0, 1], \quad u(0) = u(1) = 0$$

We perform a **parallel Schwarz iteration**:

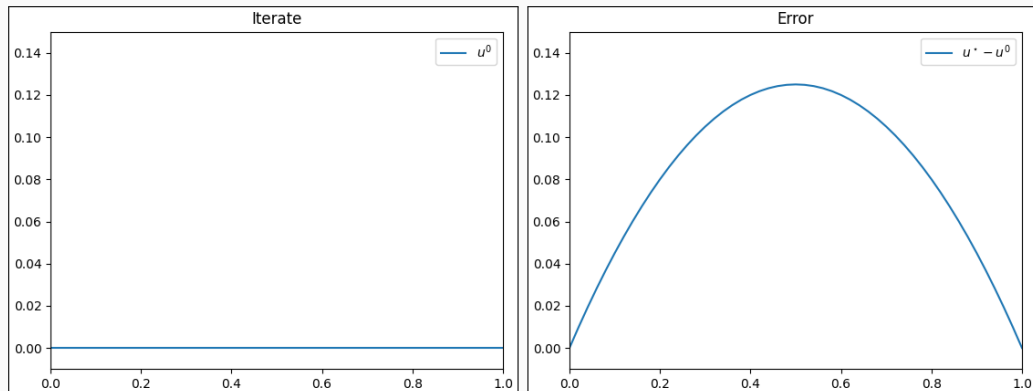


**Figure 2:** Iterate (left) and error (right) in iteration 0.

Let us again consider the simple boundary value problem: Find  $u$  such that

$$-u'' = 1, \text{ in } [0, 1], \quad u(0) = u(1) = 0$$

We perform a **parallel Schwarz iteration**:

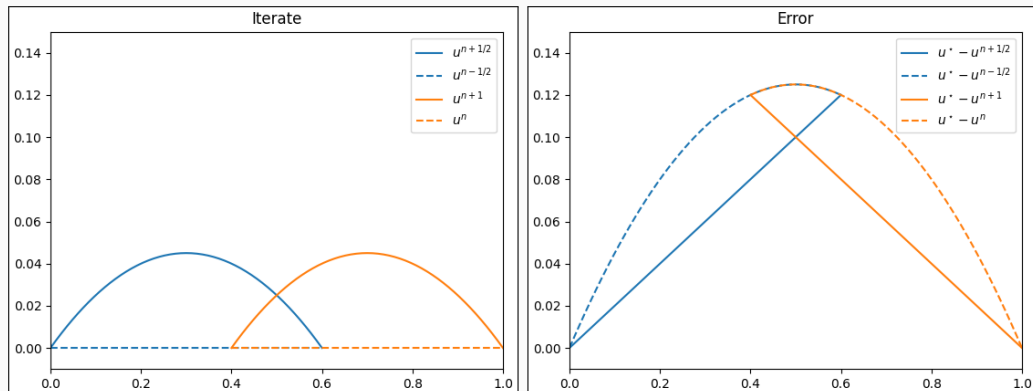


**Figure 2:** Iterate (left) and error (right) in iteration 1.

Let us again consider the simple boundary value problem: Find  $u$  such that

$$-u'' = 1, \text{ in } [0, 1], \quad u(0) = u(1) = 0$$

We perform a **parallel Schwarz iteration**:

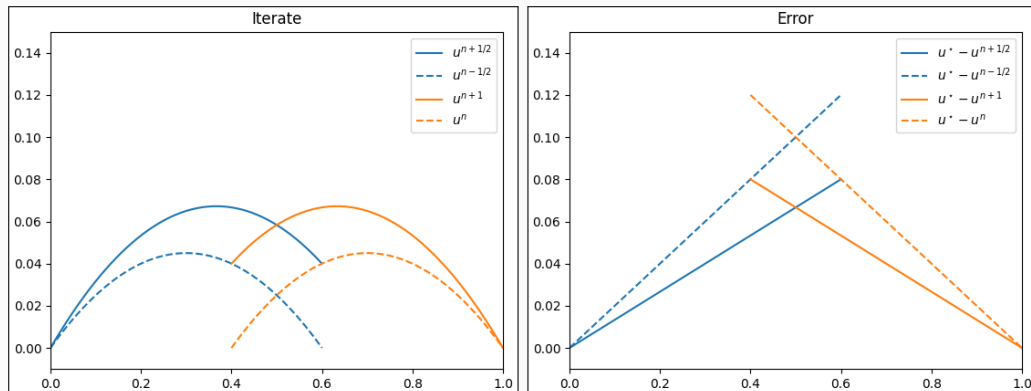


**Figure 2:** Iterate (left) and error (right) in iteration 2.

Let us again consider the simple boundary value problem: Find  $u$  such that

$$-u'' = 1, \text{ in } [0, 1], \quad u(0) = u(1) = 0$$

We perform a **parallel Schwarz iteration**:

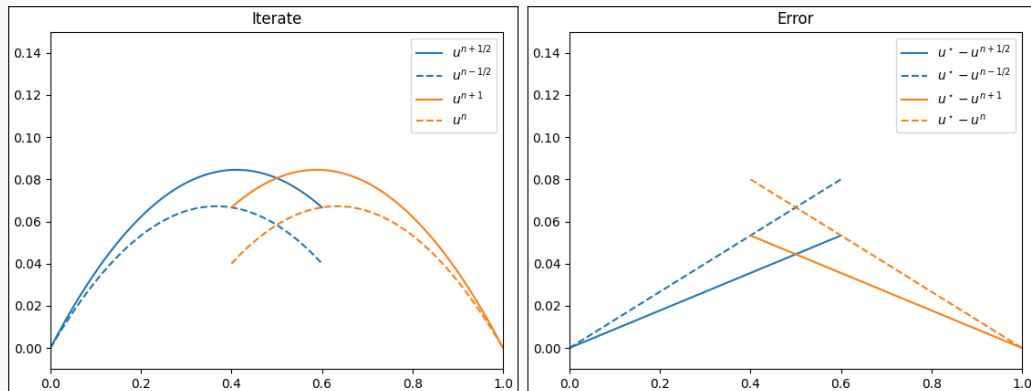


**Figure 2:** Iterate (left) and error (right) in iteration 3.

Let us again consider the simple boundary value problem: Find  $u$  such that

$$-u'' = 1, \text{ in } [0, 1], \quad u(0) = u(1) = 0$$

We perform a **parallel Schwarz iteration**:

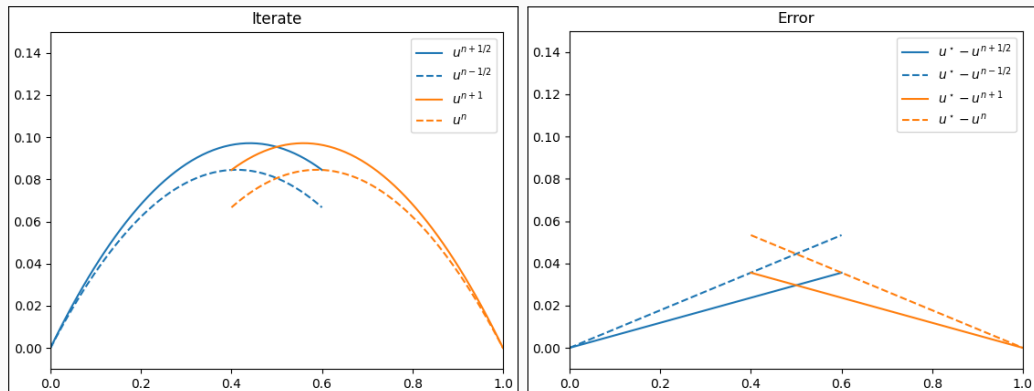


**Figure 2:** Iterate (left) and error (right) in iteration 4.

Let us again consider the simple boundary value problem: Find  $u$  such that

$$-u'' = 1, \text{ in } [0, 1], \quad u(0) = u(1) = 0$$

We perform a **parallel Schwarz iteration**:

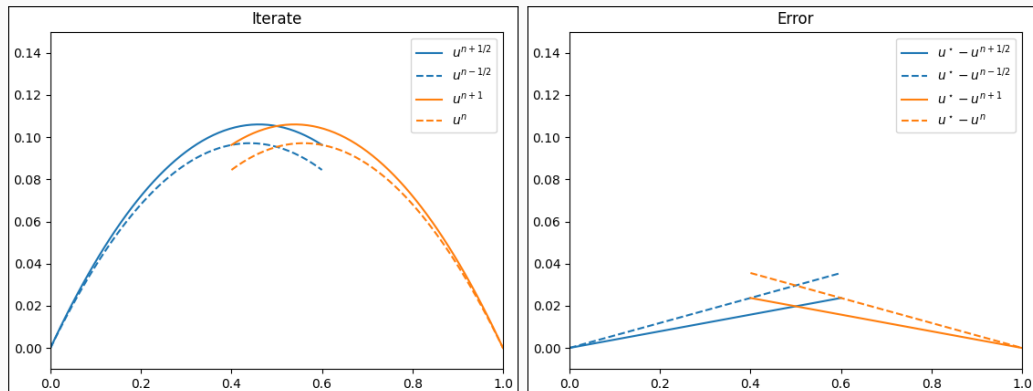
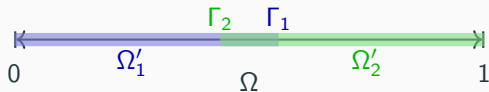


**Figure 2:** Iterate (left) and error (right) in iteration 5.

## Effect of the Size of the Overlap

We investigate the convergence of the methods (using the alternating method as an example) depending on the **size of the overlap**:

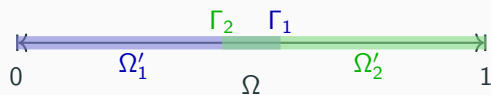


Overlap 0.05



Overlap 0.1

# Effect of the Size of the Overlap



Overlap 0.05



Overlap 0.1

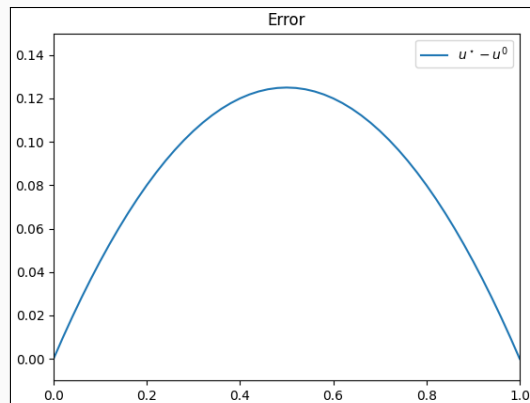
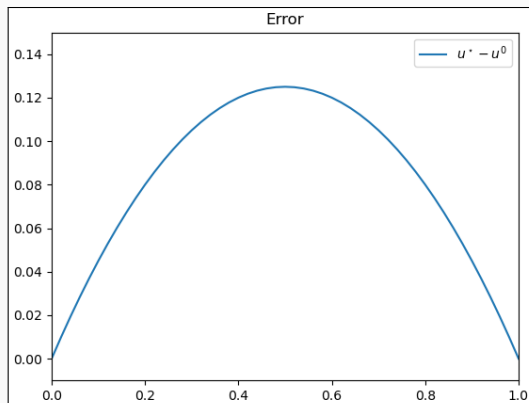
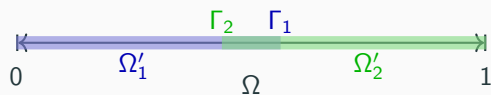


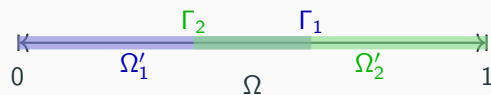
Figure 3: Error in iteration 0.



# Effect of the Size of the Overlap



Overlap 0.05



Overlap 0.1

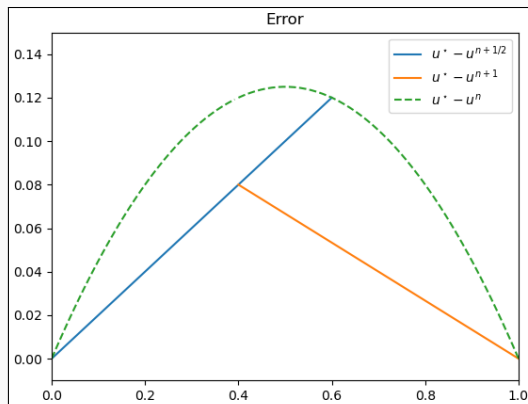
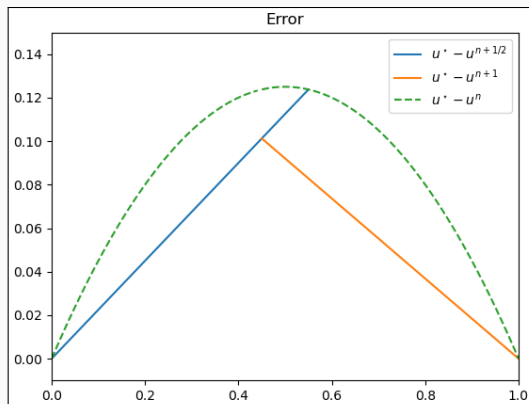
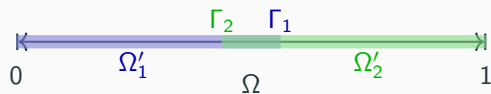
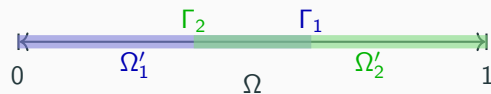


Figure 3: Error in iteration 1.

# Effect of the Size of the Overlap



Overlap 0.05



Overlap 0.1

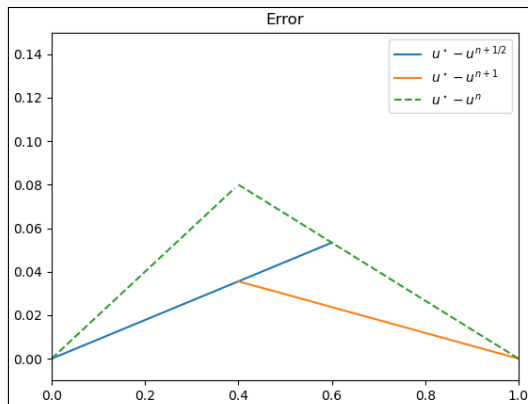
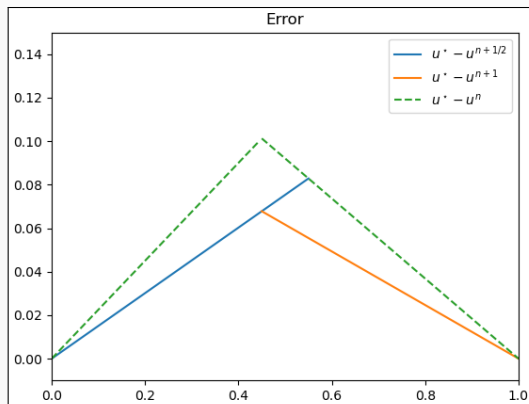


Figure 3: Error in iteration 2.

# Effect of the Size of the Overlap

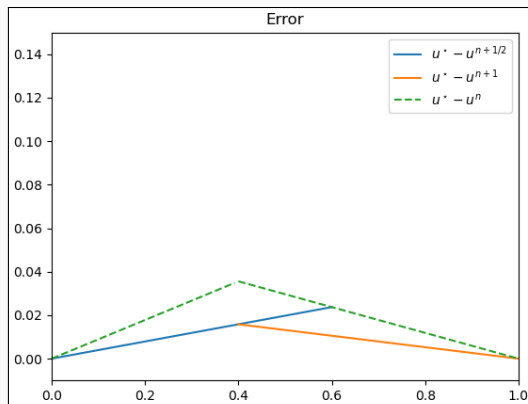
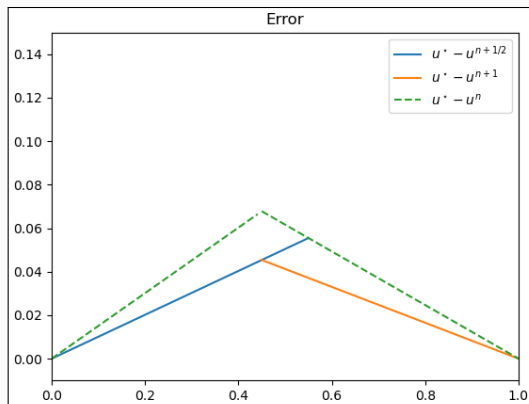
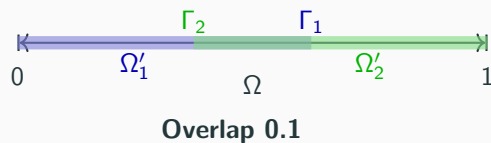
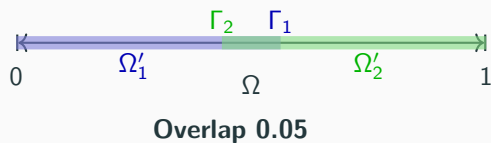


Figure 3: Error in iteration 3.

# Effect of the Size of the Overlap

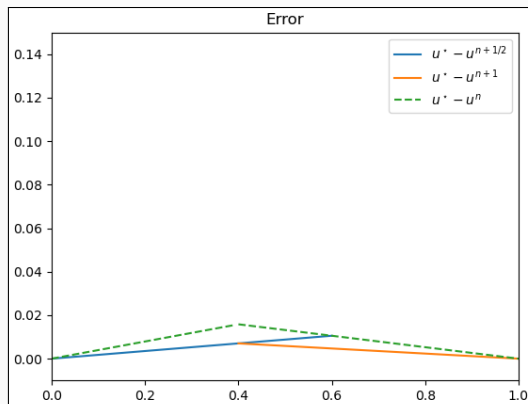
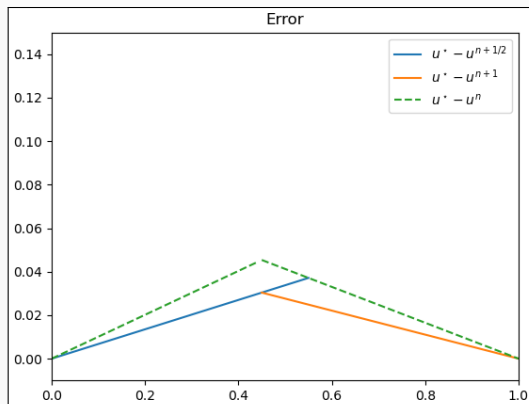
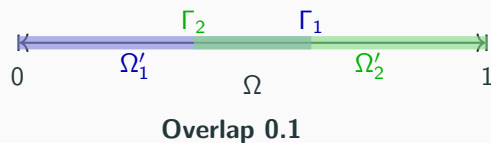
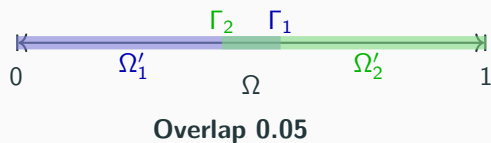
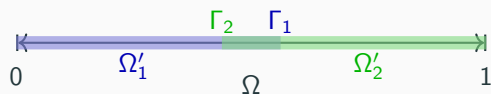


Figure 3: Error in iteration 4.

# Effect of the Size of the Overlap



Overlap 0.05



Overlap 0.1

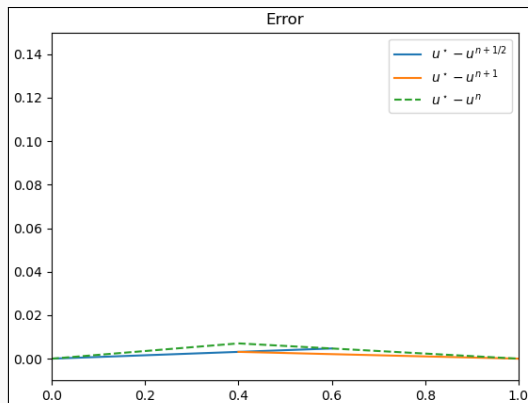
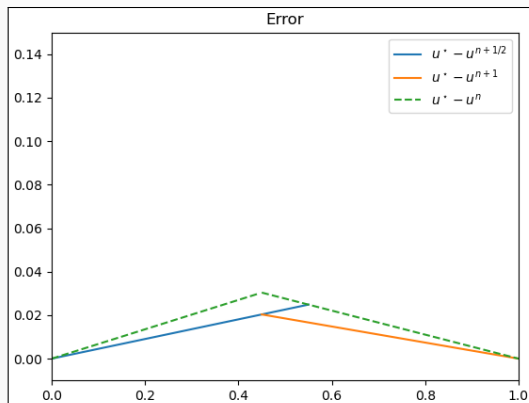
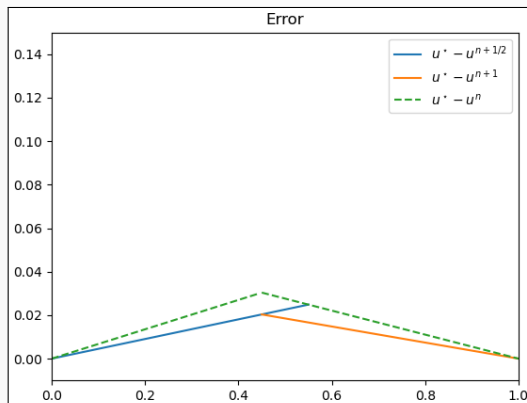


Figure 3: Error in iteration 5.

# Effect of the Size of the Overlap

## Overlap 0.05



## Overlap 0.1

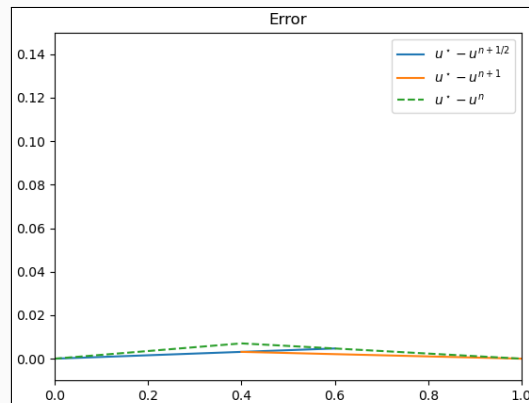


Figure 3: Error in iteration 5.

⇒ A **larger overlap** leads to **faster convergence**.

# Schwarz Domain Decomposition Preconditioners

---

# Solvers for Partial Differential Equations

Consider a **diffusion model problem**:

$$\begin{aligned} -\Delta u(x) &= f \quad \text{in } \Omega = [0, 1]^2, \\ u &= 0 \quad \text{on } \partial\Omega. \end{aligned}$$

Discretization using finite elements yields a **sparse** system of linear equations

$$Ku = f.$$

The accuracy of the finite element solution depends on the refinement level of the mesh  $h$ : **higher refinement**  $\Rightarrow$  **better accuracy**.

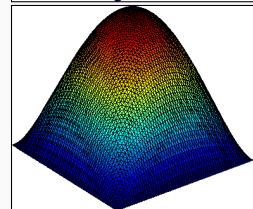
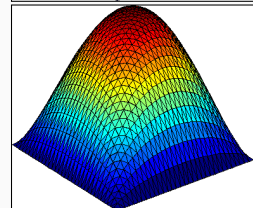
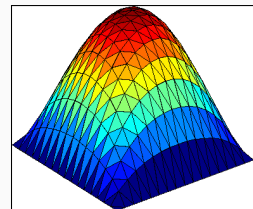
## Direct solvers

For fine meshes, solving the system using a direct solver is not feasible due to **superlinear complexity and memory cost**.

## Iterative solvers

**Iterative solvers are efficient** for solving **sparse systems**, however, the **convergence rate depends on the condition number**:

$$\kappa(K) = \frac{\lambda_{\max}(K)}{\lambda_{\min}(K)} \leq \frac{C}{h^2}$$



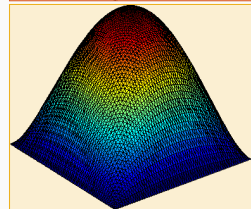
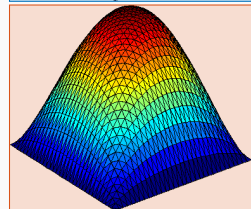
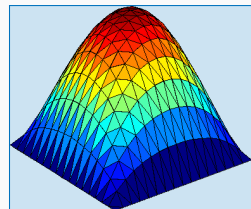
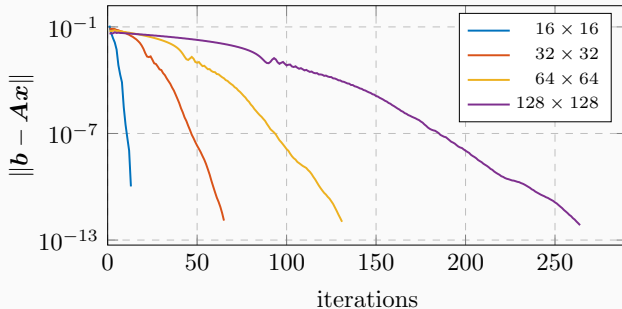


# Solvers for Partial Differential Equations

Consider a **diffusion model problem**:

$$\begin{aligned} -\Delta u(x) &= f \quad \text{in } \Omega = [0, 1]^2, \\ u &= 0 \quad \text{on } \partial\Omega. \end{aligned}$$

We solve  $Ku = f$  using the **conjugate gradient (CG) method**:

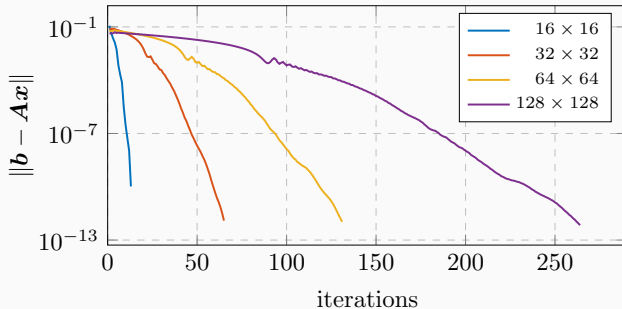


# Solvers for Partial Differential Equations

Consider a **diffusion model problem**:

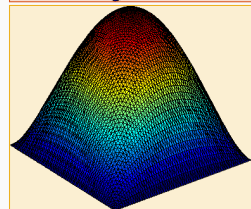
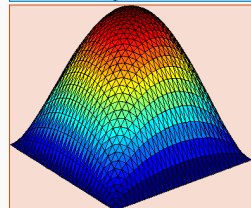
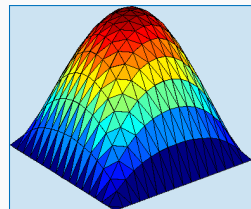
$$\begin{aligned} -\Delta u(x) &= f \quad \text{in } \Omega = [0, 1]^2, \\ u &= 0 \quad \text{on } \partial\Omega. \end{aligned}$$

We solve  $Ku = f$  using the **conjugate gradient (CG) method**:



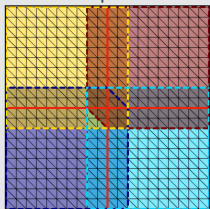
⇒ Introduce a preconditioner  $M^{-1} \approx K^{-1}$  to **improve convergence**:

$$M^{-1}Ku = M^{-1}f$$

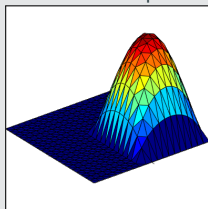


## One-level Schwarz preconditioner

Overlap  $\delta = 1h$



Solution of local problem



Based on an **overlapping domain decomposition**, we define a **one-level Schwarz operator**

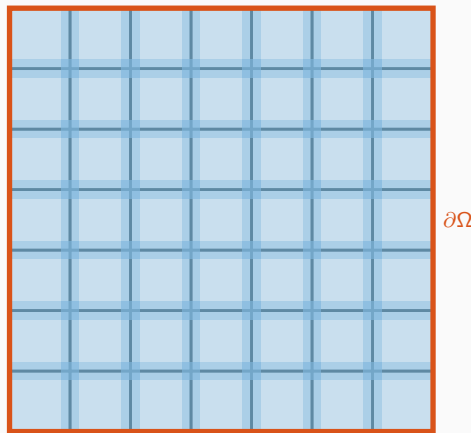
$$M_{OS-1}^{-1}K = \sum_{i=1}^N R_i^\top K_i^{-1} R_i K,$$

where  $R_i$  and  $R_i^\top$  are restriction and prolongation operators corresponding to  $\Omega'_i$ , and  $K_i := R_i K R_i^\top$ .

**Condition number estimate:**

$$\kappa(M_{OS-1}^{-1}K) \leq C \left(1 + \frac{1}{H\delta}\right)$$

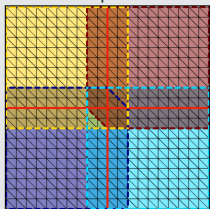
with subdomain size  $H$  and overlap width  $\delta$ .



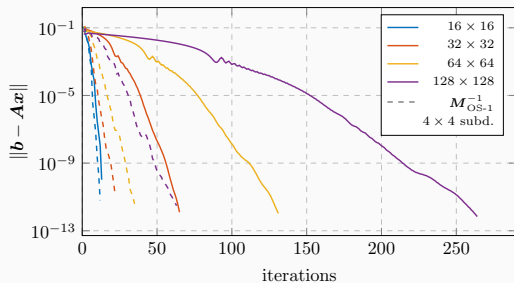
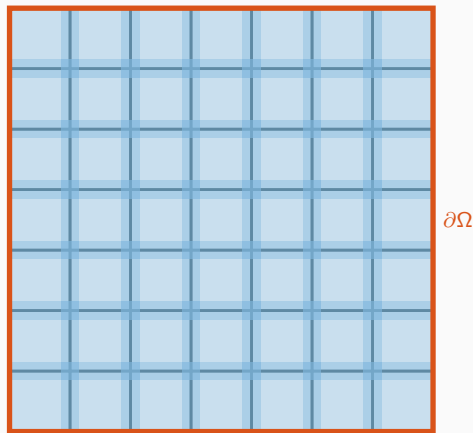
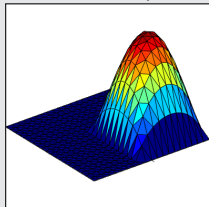
# Two-Level Schwarz Preconditioners

## One-level Schwarz preconditioner

Overlap  $\delta = 1h$



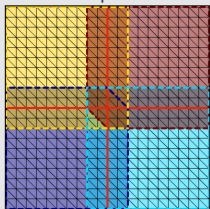
Solution of local problem



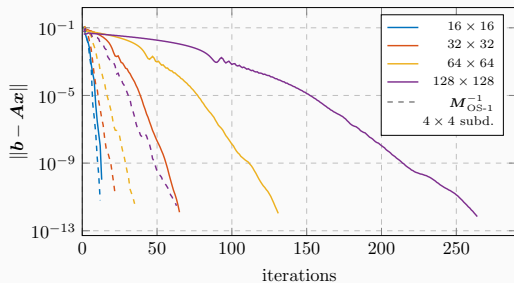
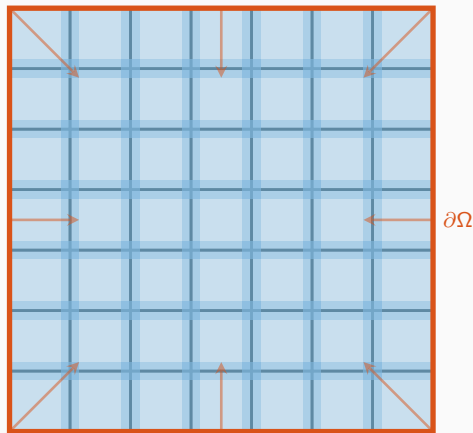
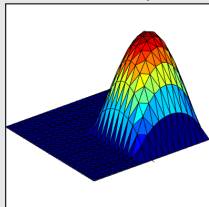
# Two-Level Schwarz Preconditioners

## One-level Schwarz preconditioner

Overlap  $\delta = 1h$



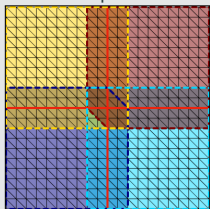
Solution of local problem



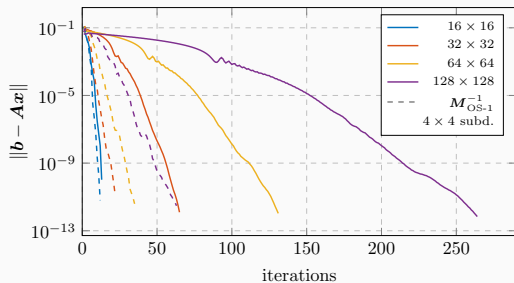
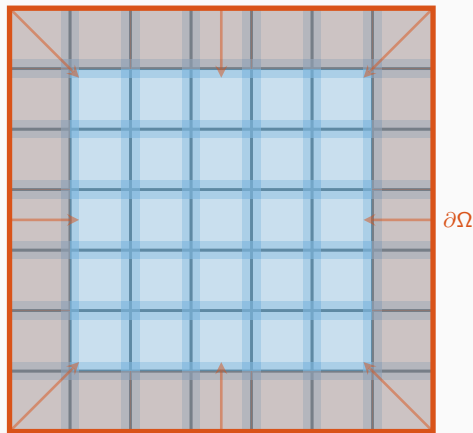
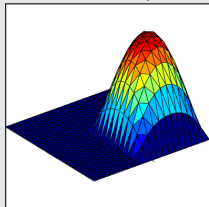
# Two-Level Schwarz Preconditioners

## One-level Schwarz preconditioner

Overlap  $\delta = 1h$



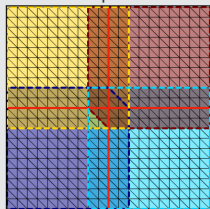
Solution of local problem



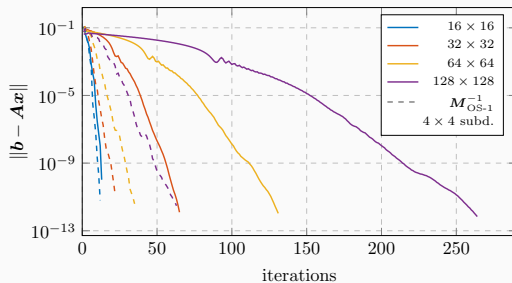
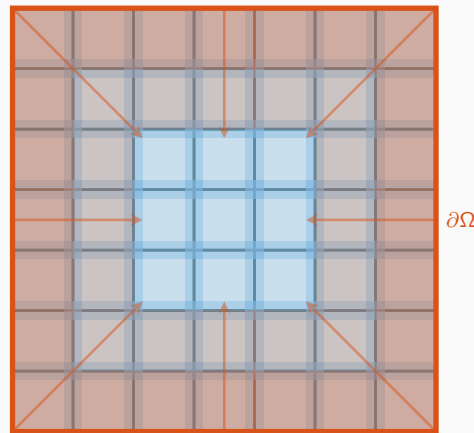
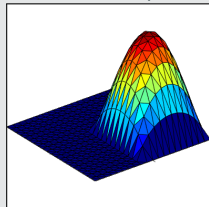
# Two-Level Schwarz Preconditioners

## One-level Schwarz preconditioner

Overlap  $\delta = 1h$



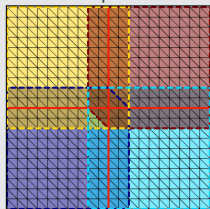
Solution of local problem



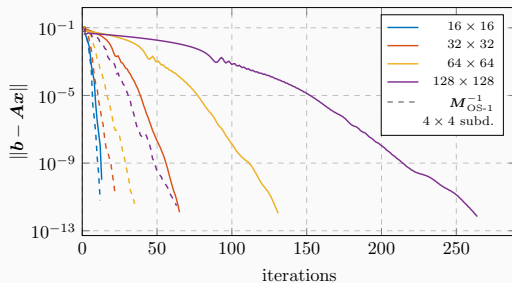
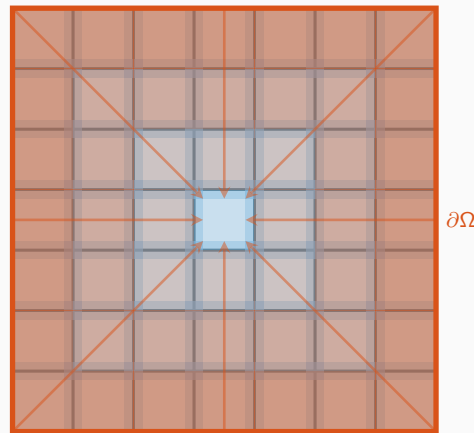
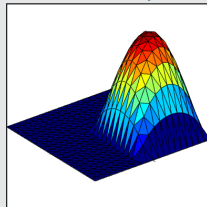
# Two-Level Schwarz Preconditioners

## One-level Schwarz preconditioner

Overlap  $\delta = 1h$



Solution of local problem

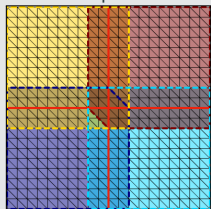




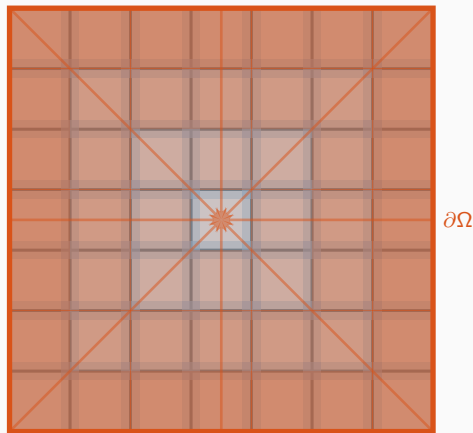
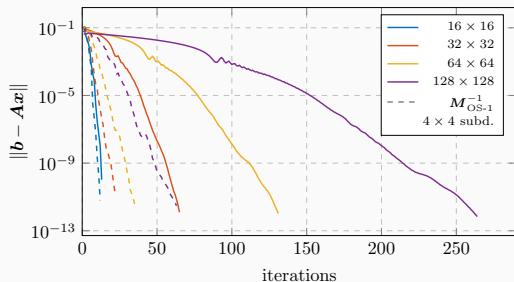
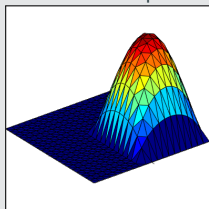
# Two-Level Schwarz Preconditioners

## One-level Schwarz preconditioner

Overlap  $\delta = 1h$



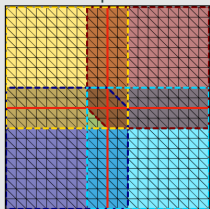
Solution of local problem



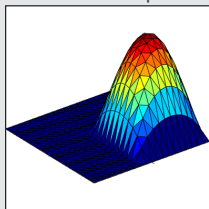
Information (in particular, boundary data) is **only** exchanged via the overlapping regions, leading to **slow convergence**  $\rightarrow$  establish a **faster / global** transport of information.

## One-level Schwarz preconditioner

Overlap  $\delta = 1h$



Solution of local problem



Based on an **overlapping domain decomposition**, we define a **one-level Schwarz operator**

$$M_{OS-1}^{-1}K = \sum_{i=1}^N R_i^\top K_i^{-1} R_i K,$$

where  $R_i$  and  $R_i^\top$  are restriction and prolongation operators corresponding to  $\Omega'_i$ , and  $K_i := R_i K R_i^\top$ .

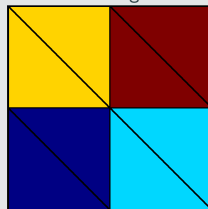
**Condition number estimate:**

$$\kappa(M_{OS-1}^{-1}K) \leq C \left(1 + \frac{1}{H\delta}\right)$$

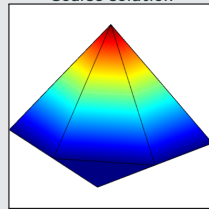
with subdomain size  $H$  and overlap width  $\delta$ .

## Lagrangian coarse space

Coarse triangulation



Coarse solution



The **two-level overlapping Schwarz operator** reads

$$M_{OS-2}^{-1}K = \underbrace{\Phi K_0^{-1} \Phi^\top K}_{\text{coarse level - global}} + \underbrace{\sum_{i=1}^N R_i^\top K_i^{-1} R_i K}_{\text{first level - local}},$$

where  $\Phi$  contains the coarse basis functions and  $K_0 := \Phi^\top K \Phi$ ; cf., e.g., **Toselli, Widlund (2005)**.

The construction of a Lagrangian coarse basis requires a coarse triangulation.

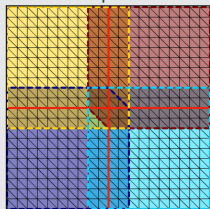
**Condition number estimate:**

$$\kappa(M_{OS-2}^{-1}K) \leq C \left(1 + \frac{H}{\delta}\right)$$

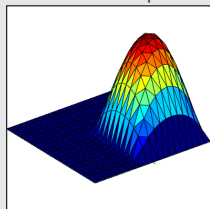
# Two-Level Schwarz Preconditioners

## One-level Schwarz preconditioner

Overlap  $\delta = 1h$

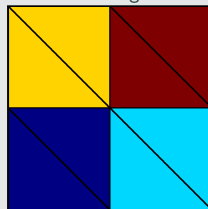


Solution of local problem

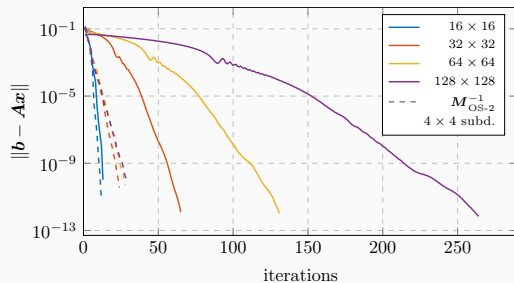
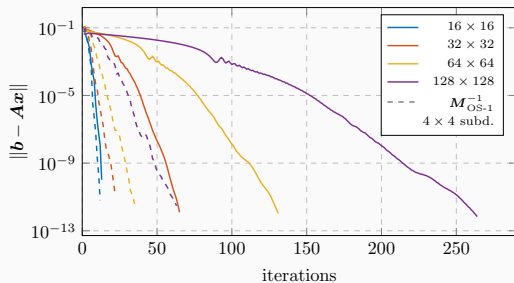
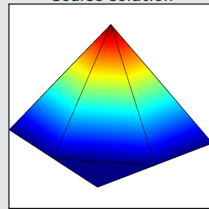


## Lagrangian coarse space

Coarse triangulation



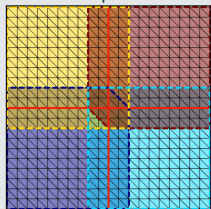
Coarse solution



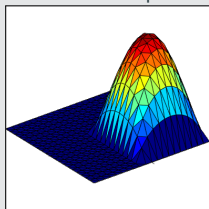
# Two-Level Schwarz Preconditioners

## One-level Schwarz preconditioner

Overlap  $\delta = 1h$

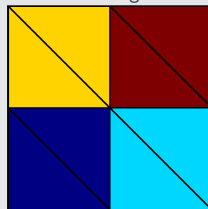


Solution of local problem

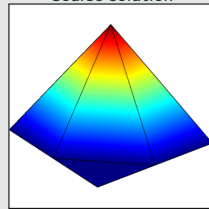


## Lagrangian coarse space

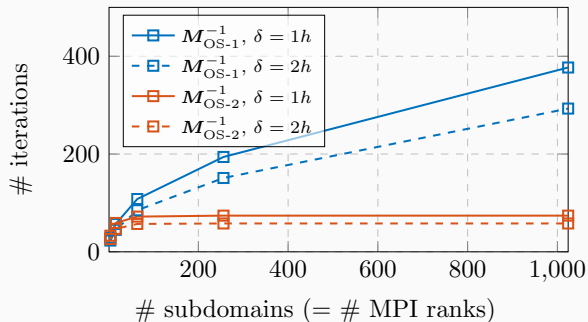
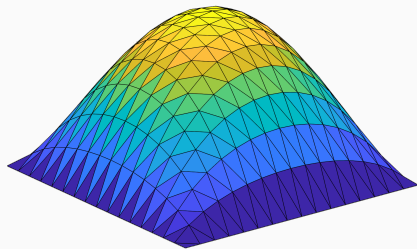
Coarse triangulation



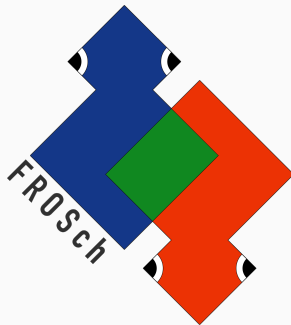
Coarse solution



Diffusion model problem in two dimensions,  
 $H/h = 100$



# FROSch (Fast and Robust Overlapping Schwarz) Framework in Trilinos



Sandia  
National  
Laboratories



TUBAF  
Die Ressourcenuniversität.  
Seit 1765.

## Software

- Object-oriented C++ domain decomposition solver framework with MPI-based distributed memory parallelization
- Part of TRILINOS with support for both parallel linear algebra packages EPETRA and TPETRA
- Node-level parallelization and performance portability on CPU and GPU architectures through KOKKOS and KOKKOSKERNELS
- Accessible through unified TRILINOS solver interface STRATIMIKOS

## Methodology

- **Parallel scalable multi-level Schwarz domain decomposition preconditioners**
- **Algebraic construction** based on the parallel distributed system matrix
- **Extension-based coarse spaces**

## Team (active)

- Filipe Cumaru (TU Delft)
- Kyrill Ho (UCologne)
- Jascha Knepper (UCologne)
- Friederike Röver (TUBAF)
- Lea Saßmannshausen (UCologne)
- Alexander Heinlein (TU Delft)
- Axel Klawonn (UCologne)
- Siva Rajamanickam (SNL)
- Oliver Rheinbach (TUBAF)
- Ichitaro Yamazaki (SNL)

## Overlapping domain decomposition

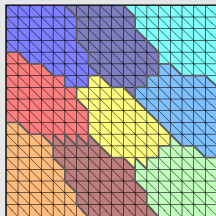
The **overlapping subdomains** are constructed by **recursively adding layers of elements** via the sparsity pattern of  $K$ .

The corresponding matrices

$$K_i = R_i K R_i^T$$

can easily be extracted from  $K$ .

### Nonoverlapping DD



## Overlapping domain decomposition

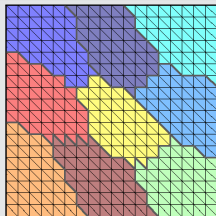
The **overlapping subdomains** are constructed by **recursively adding layers of elements** via the sparsity pattern of  $K$ .

The corresponding matrices

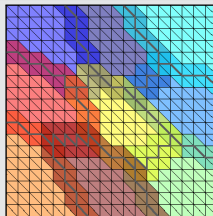
$$K_i = R_i K R_i^T$$

can easily be extracted from  $K$ .

Nonoverlapping DD



Overlap  $\delta = 1h$



## Overlapping domain decomposition

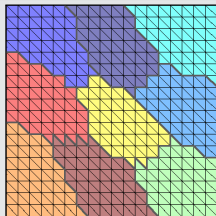
The **overlapping subdomains** are constructed by **recursively adding layers of elements** via the sparsity pattern of  $\mathbf{K}$ .

The corresponding matrices

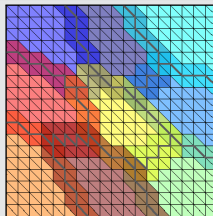
$$\mathbf{K}_i = \mathbf{R}_i \mathbf{K} \mathbf{R}_i^T$$

can easily be extracted from  $\mathbf{K}$ .

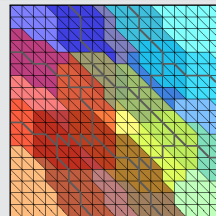
Nonoverlapping DD



Overlap  $\delta = 1h$



Overlap  $\delta = 2h$





## Overlapping domain decomposition

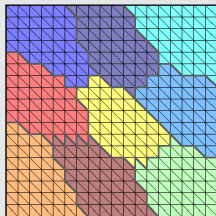
The **overlapping subdomains** are constructed by **recursively adding layers of elements** via the sparsity pattern of  $K$ .

The corresponding matrices

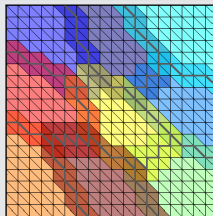
$$K_i = R_i K R_i^T$$

can easily be extracted from  $K$ .

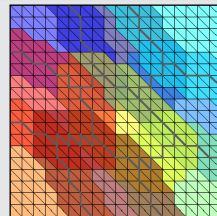
Nonoverlapping DD



Overlap  $\delta = 1h$

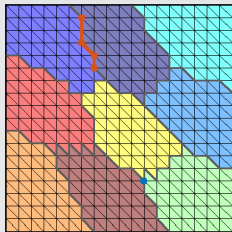


Overlap  $\delta = 2h$



## Coarse space – Example of Generalized Dryja–Smith–Widlund (GDSW)

### 1. Interface components



## Overlapping domain decomposition

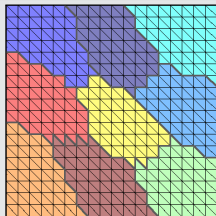
The **overlapping subdomains** are constructed by **recursively adding layers of elements** via the sparsity pattern of  $K$ .

The corresponding matrices

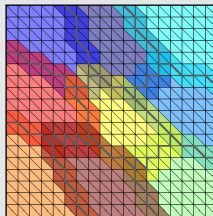
$$K_i = R_i K R_i^T$$

can easily be extracted from  $K$ .

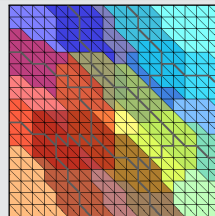
Nonoverlapping DD



Overlap  $\delta = 1h$

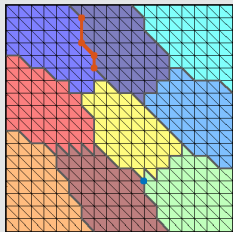


Overlap  $\delta = 2h$

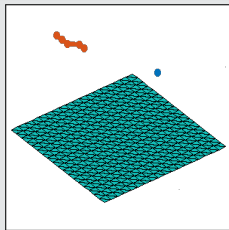


## Coarse space – Example of Generalized Dryja–Smith–Widlund (GDSW)

### 1. Interface components



### 2. Interface basis (partition of unity $\times$ null space)



For scalar elliptic problems, the null space consists only of constant functions.

# Algorithmic Framework for FROSch Preconditioners

## Overlapping domain decomposition

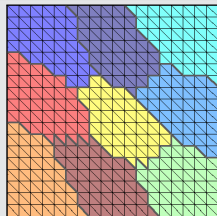
The **overlapping subdomains** are constructed by **recursively adding layers of elements** via the sparsity pattern of  $K$ .

The corresponding matrices

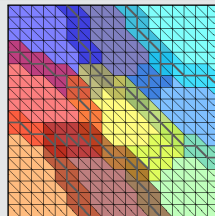
$$K_i = R_i K R_i^T$$

can easily be extracted from  $K$ .

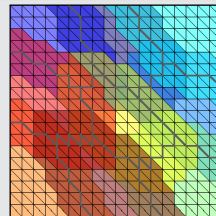
Nonoverlapping DD



Overlap  $\delta = 1h$

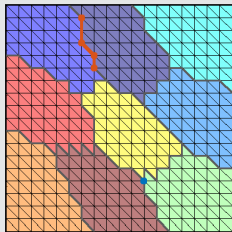


Overlap  $\delta = 2h$

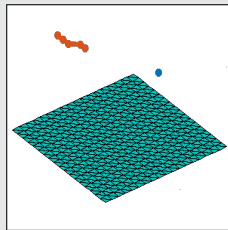


## Coarse space – Example of Generalized Dryja–Smith–Widlund (GDSW)

1. Interface components

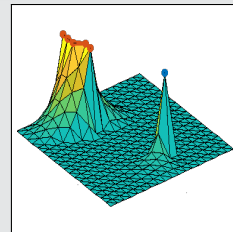


2. Interface basis (partition of unity  $\times$  null space)



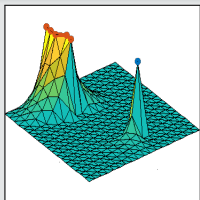
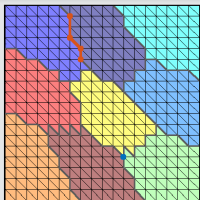
For scalar elliptic problems, the null space consists only of constant functions.

3. Extension



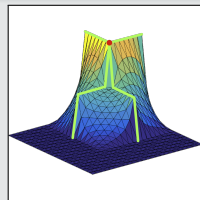
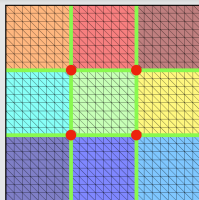
# Examples of FROSch Coarse Spaces

## GDSW (Generalized Dryja–Smith–Widlund)



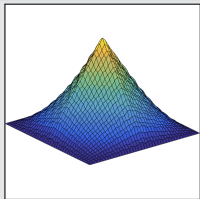
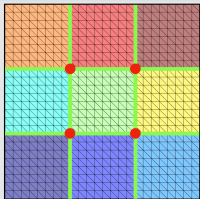
- Dohrmann, Klawonn, Widlund (2008)
- Dohrmann, Widlund (2009, 2010, 2012)

## RGDSW (Reduced dimension GDSW)



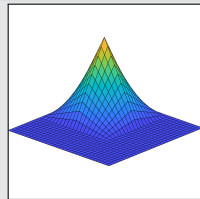
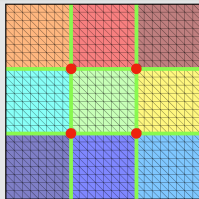
- Dohrmann, Widlund (2017)
- H., Klawonn, Knepper, Rheinbach, Widlund (2022)

## MsFEM (Multiscale Finite Element Method)



- Hou (1997), Efendiev and Hou (2009)
- Buck, Iliev, and Andrä (2013)
- H., Klawonn, Knepper, Rheinbach (2018)

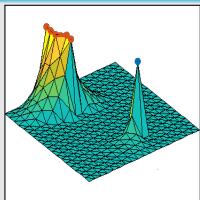
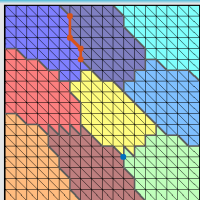
## Q1 Lagrangian / piecewise bilinear



Piecewise linear interface partition of unity functions and a structured domain decomposition.

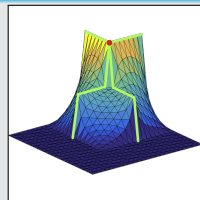
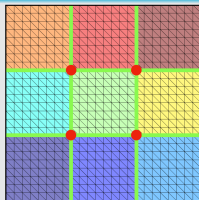
# Examples of FROSch Coarse Spaces

## GDSW (Generalized Dryja–Smith–Widlund)



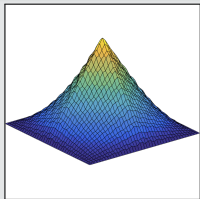
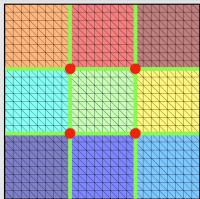
- Dohrmann, Klawonn, Widlund (2008)
- Dohrmann, Widlund (2009, 2010, 2012)

## RGDSW (Reduced dimension GDSW)



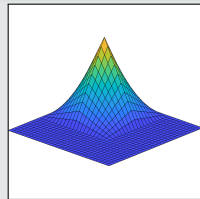
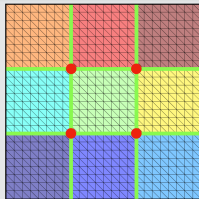
- Dohrmann, Widlund (2017)
- H., Klawonn, Knepper, Rheinbach, Widlund (2022)

## MsFEM (Multiscale Finite Element Method)



- Hou (1997), Efendiev and Hou (2009)
- Buck, Iliev, and Andrä (2013)
- H., Klawonn, Knepper, Rheinbach (2018)

## Q1 Lagrangian / piecewise bilinear

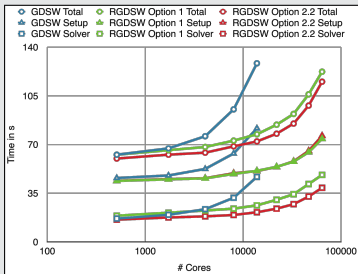
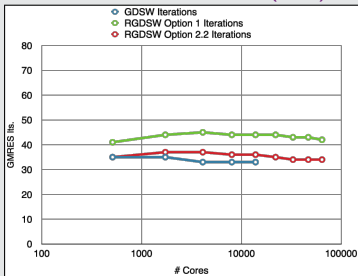


Piecewise linear interface partition of unity functions and a structured domain decomposition.

# Weak Scalability up to 64k MPI Ranks / 1.7b Unknowns (3D Poisson; Juqueen)

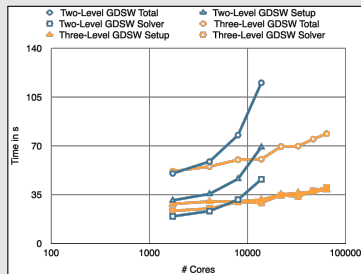
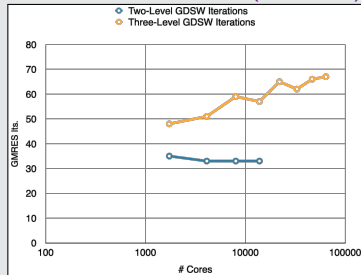
## GDSW vs RGDSW (reduced dimension)

Heinlein, Klawonn, Rheinbach, Widlund (2019).



## Two-level vs three-level GDSW

Heinlein, Klawonn, Rheinbach, Röver (2019, 2020).



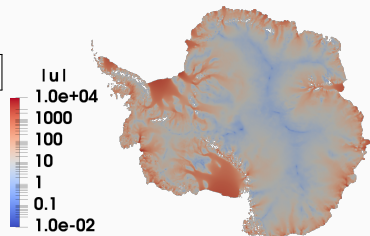


<https://github.com/SNLComputation/Albany>

The velocity of the ice sheet in Antarctica and Greenland is modeled by a **first-order-accurate Stokes approximation model**,

$$-\nabla \cdot (2\mu\dot{\epsilon}_1) + \rho g \frac{\partial s}{\partial x} = 0, \quad -\nabla \cdot (2\mu\dot{\epsilon}_2) + \rho g \frac{\partial s}{\partial y} = 0,$$

with a **nonlinear viscosity model** (Glen's law); cf., e.g., **Blatter (1995)** and **Pattyn (2003)**.



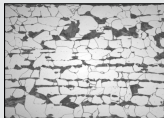
MPI ranks	Antarctica ( <b>velocity</b> )			Greenland ( <b>multiphysics vel. &amp; temperature</b> )		
	4 km resolution, 20 layers, 35 m dofs			1-10 km resolution, 20 layers, 69 m dofs		
	avg. its	avg. setup	avg. solve	avg. its	avg. setup	avg. solve
512	<b>41.9</b> (11)	25.10 s	12.29 s	<b>41.3</b> (36)	18.78 s	4.99 s
1 024	<b>43.3</b> (11)	9.18 s	5.85 s	<b>53.0</b> (29)	8.68 s	4.22 s
2 048	<b>41.4</b> (11)	4.15 s	2.63 s	<b>62.2</b> (86)	4.47 s	4.23 s
4 096	<b>41.2</b> (11)	1.66 s	1.49 s	<b>68.9</b> (40)	2.52 s	2.86 s
8 192	<b>40.2</b> (11)	1.26 s	1.06 s	-	-	-

Computations performed on Cori (NERSC).

**Heinlein, Perego, Rajamanickam (2022)**

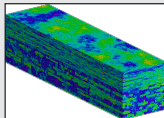
## Highly heterogeneous problems ...

... appear in most areas of modern science and engineering:

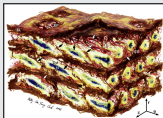


Micro section of a dual-phase steel.

Courtesy of J. Schröder.



Groundwater flow (SPE10);  
cf. Christie and Blunt (2001).



Composition of arterial walls; taken from O'Connell et al. (2008).

## Spectral coarse spaces

The coarse space is **enhanced** by eigenfunctions of **local edge and face eigenvalue problems** with eigenvalues below tolerances  $tol_g$  and  $tol_f$ :

$$\kappa(M_*^{-1}K) \leq C \left( 1 + \frac{1}{tol_g} + \frac{1}{tol_f} + \frac{1}{tol_g \cdot tol_f} \right);$$

$C$  does not depend on  $h$ ,  $H$ , or the coefficients.

**OS-ACMS** & **adaptive GDSW (AGDSW)** (Heinlein, Klawonn, Knepper, Rheinbach (2018, 2018, 2019)).

## Related works (non-exhaustive)

- **FETI & Neumann–Neumann**: Bjørstad, Krzyzanowski (2002); Bjørstad, Koster, Krzyzanowski (2001); Rixen, Spillane (2013); Spillane (2015, 2016) ...
- **BDDC & FETI-DP**: Mandel, Sousedik (2007); Sousedik (2010); Sístek, Mandel, Sousedik (2012); Dohrmann, Pechstein (2013, 2016); Klawonn, Radtke, Rheinbach (2014, 2015, 2016); Klawonn, Kühn, Rheinbach (2015, 2016, 2017); Kim, Chung (2015); Kim, Chung, Wang (2017); Beirão da Veiga et al. (2017); Calvo, Widlund (2016); Oh et al. (2017) ...
- **Overlapping Schwarz**: Galvis, Efendiev (2010, 2011); Nataf, Xiang, Dolean, Spillane (2011); Spillane et al. (2011); Gander, Loneland, Rahman (preprint 2015); Eikeland, Marcinkowski, Rahman (TR 2016); Marcinkowski, Rahman (2018), Al Daas, Grigori, Jolivet, Tournier (2021); Bastian, Scheichl, Seelinger, Strehlow (2022); Spillane (preprint 2021, acc. 2024); Al Daas, Jolivet (2022); Bootland, Dolean, Graham, Ma, Scheichl (2023) ...
- **Spectral AMGe ( $\rho$ AMGe)**: Chartier, Falgout, Henson, Jones, Manteuffel, McCormick, Ruge, Vassilevski (2003) ...



# Spectral Extension-Based Coarse Spaces for Schwarz Preconditioners

## Local eigenvalue problems

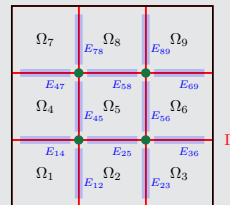
Local generalized eigenvalue problems corresponding to the edges  $\mathcal{E}$  and faces  $\mathcal{F}$  of the domain decomposition:

$$\forall E \in \mathcal{E} : \quad \mathbf{S}_{EE} \mathbf{T}_{*,E} = \lambda_{*,E} \mathbf{K}_{EE} \mathbf{T}_{*,E}, \quad \forall \mathbf{T}_{*,E} \in V_E,$$

$$\forall F \in \mathcal{F} : \quad \mathbf{S}_{FF} \mathbf{T}_{*,F} = \lambda_{*,F} \mathbf{K}_{FF} \mathbf{T}_{*,F}, \quad \forall \mathbf{T}_{*,F} \in V_F,$$

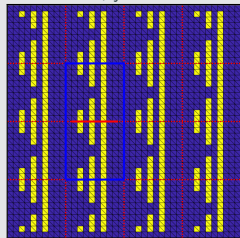
with **Schur complements**  $\mathbf{S}_{EE}$ ,  $\mathbf{S}_{FF}$  with **Neumann boundary conditions** and **submatrices**  $\mathbf{K}_{EE}$ ,  $\mathbf{K}_{FF}$  of  $\mathbf{K}$ . We select eigenfunctions corresponding to **eigenvalues below tolerances**  $tol_{\mathcal{E}}$  and  $tol_{\mathcal{F}}$ .

→ The corresponding coarse basis functions are **energy-minimizing extensions** into the interior of the subdomains.

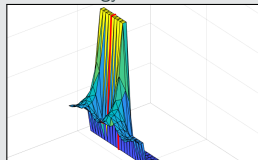


## Extensions in the generalized eigenvalue problem

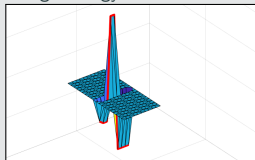
Blue  $\alpha = 1$ ; yellow  $\alpha = 10^6$



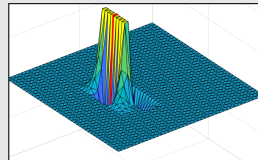
Low energy extension  $\mathbf{S}_{EE}$



High energy extension  $\mathbf{K}_{EE}$



Coarse basis function

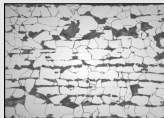


The extensions on the two sides of the generalized eigenvalue problem correspond to **low and high energy extensions of the trace** → detects coefficient jumps.

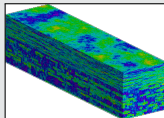
# Spectral Extension-Based Coarse Spaces for Schwarz Preconditioners

## Highly heterogeneous problems ...

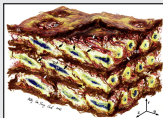
... appear in most areas of modern science and engineering:



Micro section of a dual-phase steel.  
Courtesy of J. Schröder.



Groundwater flow (SPE10);  
cf. Christie and Blunt (2001).



Composition of arterial walls; taken from O'Connell et al. (2008).

## Spectral coarse spaces

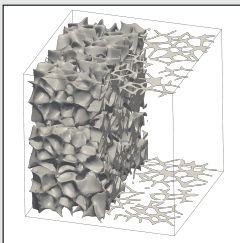
The coarse space is **enhanced** by eigenfunctions of **local edge and face eigenvalue problems** with eigenvalues below tolerances  $tol_{\mathcal{E}}$  and  $tol_{\mathcal{F}}$ :

$$\kappa(M_*^{-1}K) \leq C \left( 1 + \frac{1}{tol_{\mathcal{E}}} + \frac{1}{tol_{\mathcal{F}}} + \frac{1}{tol_{\mathcal{E}} \cdot tol_{\mathcal{F}}} \right);$$

$C$  does not depend on  $h$ ,  $H$ , or the coefficients.

**OS-ACMS** & **adaptive GDSW (AGDSW)** (Heinlein, Klawonn, Knepper, Rheinbach (2018, 2018, 2019)).

## Foam coefficient function example



Solid phase:  $\alpha = 10^6$ ; transparent phase:  $\alpha = 1$ ; 100 subdomains

$V_0$	$tol_{\mathcal{E}}$	$tol_{\mathcal{F}}$	it.	$\kappa$	dim $V_0$	dim $V_0$ / dof
$V_{\text{GDSW}}$	—	—	565	$1.3 \cdot 10^6$	1 601	0.27 %
$V_{\text{AGDSW}}$	0.05	0.05	60	30.2	1 968	0.33 %
$V_{\text{OS-ACMS}}$	0.001	0.001	57	30.3	690	0.12 %

Cf. Heinlein, Klawonn, Knepper, Rheinbach (2018, 2019).

# Algebraic Spectral Extension-Based Coarse Spaces

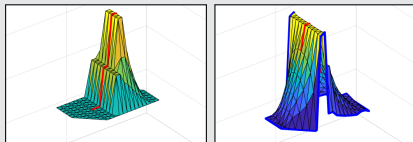
## Two algebraic eigenvalue problems

Use the  $a$ -orthogonal decomposition

$$V_{\Omega_e} = V_{\Omega_e}^0 \oplus \{E_{\partial\Omega_e \rightarrow \Omega_e}(v) : v \in V_{\partial\Omega_e}\}$$

to “split the AGDSW (Neumann) eigenvalue problem” into two:

- Dirichlet eigenvalue problem on  $V_{\Omega_e}^0$
- Transfer eigenvalue problem on  $V_{\Omega_e, \text{harm}}$ ; cf. [Smetana, Patera \(2016\)](#)



## Condition number estimate

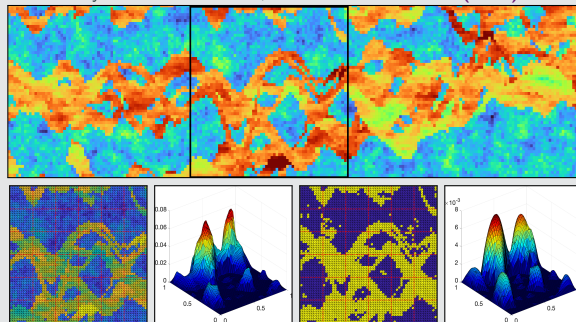
$$\kappa \left( \mathbf{M}_{\text{DIR\&TR}}^{-1} \mathbf{K} \right) \leq C \max \{1/TOL_{\text{DIR}}, TOL_{\text{TR}}/\alpha_{\min}\},$$

where  $C$  is independent of  $H$ ,  $h$ , and the contrast of the coefficient function  $\alpha$ .

[Heinlein & Smetana \(acc. 2024; preprint arXiv\)](#).

## Numerical results – SPE10 benchmark

Layer 70 from model 2; cf. [Christie and Blunt \(2001\)](#)



$V_0$	$TOL_{\text{DIR}}$	$TOL_{\text{TR}}$	$\dim V_0$	$\kappa$	its.
$V_{\text{GDSW}}$	-	-	85	$2.0 \cdot 10^5$	57
$V_{\text{AGDSW}}$	$1.0 \cdot 10^{-2}$	-	93	19.3	38
$V_{\text{DIR\&TR}-a}$	$1.0 \cdot 10^{-3}$	$1.0 \cdot 10^5$	90	19.4	39
$V_{\text{DIR\&TR}-\rho^2}$	$1.0 \cdot 10^{-3}$	$1.0 \cdot 10^5$	147	9.6	31
Original coefficient (without thresholding)					
$V_{\text{GDSW}}$	-	-	85	20.6	42

# Domain Decomposition for Neural Networks

---

## A non-exhaustive literature overview:

- **Machine Learning for adaptive BDDC, FETI–DP, and AGDSW:** Heinlein, Klawonn, Lanser, Weber (2019, 2020, 2021, 2021, 2021, 2022); Klawonn, Lanser, Weber (2024)
- **cPINNs, XPINNs:** Jagtap, Kharazmi, Karniadakis (2020); Jagtap, Karniadakis (2020)
- **Classical Schwarz iteration for PINNs or DeepRitz (D3M, DeepDDM, etc):** Li, Tang, Wu, and Liao (2019); Li, Xiang, Xu (2020); Mercier, Gratton, Boudier (arXiv 2021); Dolean, Heinlein, Mercier, Gratton (subm. 2024 / arXiv:2408.12198); Li, Wang, Cui, Xiang, Xu (2023); Sun, Xu, Yi (arXiv 2022, arXiv 2023); Kim, Yang (2022, arXiv 2023)
- **FBPINNs, FBKANs:** Moseley, Markham, and Nissen-Meyer (2023); Dolean, Heinlein, Mishra, Moseley (2024, 2024); Heinlein, Howard, Beecroft, Stinis (acc. 2024 / arXiv:2401.07888); Howard, Jacob, Murphy, Heinlein, Stinis (arXiv:2406.19662)
- **DDMs for CNNs:** Gu, Zhang, Liu, Cai (2022); Lee, Park, Lee (2022); Klawonn, Lanser, Weber (2024); Verburg, Heinlein, Cyr (subm. 2024)

An overview of the state-of-the-art in early 2021:



A. Heinlein, A. Klawonn, M. Lanser, J. Weber

**Combining machine learning and domain decomposition methods for the solution of partial differential equations — A review**

GAMM-Mitteilungen. 2021.

An overview of the state-of-the-art in mid 2024:



A. Klawonn, M. Lanser, J. Weber

**Machine learning and domain decomposition methods – a survey**

Computational Science and Engineering. 2024

# Physics-Informed Neural Networks (PINNs)

In the **physics-informed neural network (PINN)** approach introduced by **Raissi et al. (2019)**, a neural network is employed to **discretize a partial differential equation**

$$\mathcal{N}[u] = f, \quad \text{in } \Omega.$$

PINNs use a **hybrid loss function**:

$$\mathcal{L}(\theta) = \omega_{\text{data}} \mathcal{L}_{\text{data}}(\theta) + \omega_{\text{PDE}} \mathcal{L}_{\text{PDE}}(\theta),$$

where  $\omega_{\text{data}}$  and  $\omega_{\text{PDE}}$  are **weights** and

$$\mathcal{L}_{\text{data}}(\theta) = \frac{1}{N_{\text{data}}} \sum_{i=1}^{N_{\text{data}}} (u(\hat{x}_i, \theta) - u_i)^2,$$

$$\mathcal{L}_{\text{PDE}}(\theta) = \frac{1}{N_{\text{PDE}}} \sum_{i=1}^{N_{\text{PDE}}} (\mathcal{N}[u](x_i, \theta) - f(x_i))^2.$$

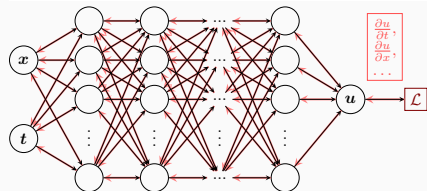
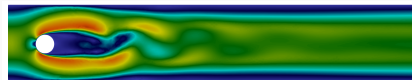
See also **Dissanayake and Phan-Thien (1994)**; **Lagaris et al. (1998)**.

## Advantages

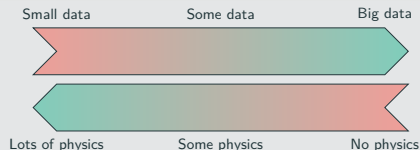
- **“Meshfree”**
- **Small data**
- **Generalization properties**
- **High-dimensional problems**
- **Inverse and parameterized problems**

## Drawbacks

- **Training cost** and **robustness**
- **Convergence not well-understood**
- **Difficulties with scalability** and **multi-scale problems**



## Hybrid loss



- **Known solution values** can be included in  $\mathcal{L}_{\text{data}}$
- **Initial and boundary conditions** are also included in  $\mathcal{L}_{\text{data}}$

# Theoretical Result for PINNs

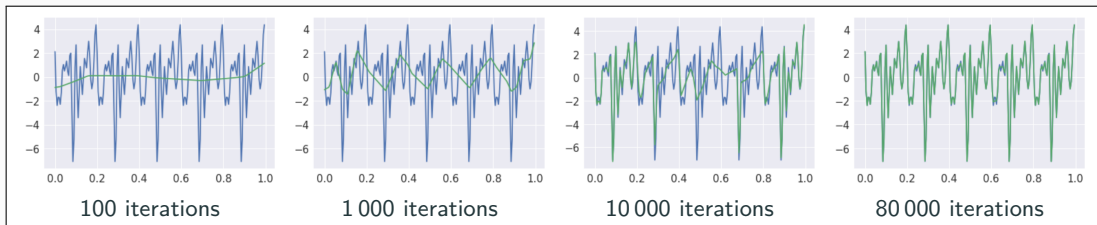
## Estimate of the generalization error (Mishra and Molinaro (2022))

The generalization error (or total error) satisfies

$$\varepsilon_G \leq C_{\text{PDE}} \varepsilon_{\mathcal{T}} + C_{\text{PDE}} C_{\text{quad}}^{1/p} N^{-\alpha/p}$$

- $\varepsilon_G = \varepsilon_G(\mathbf{X}, \theta) := \|\mathbf{u} - \mathbf{u}^*\|_V$  **general. error** ( $V$  Sobolev space,  $\mathbf{X}$  training data set)
- $\varepsilon_{\mathcal{T}}$  **training error** ( $L^p$  loss of the residual of the PDE)
- $N$  **number of the training points** and  $\alpha$  **convergence rate of the quadrature**
- $C_{\text{PDE}}$  and  $C_{\text{quad}}$  **constants** depending on the **PDE, quadrature, and neural network**

*Rule of thumb: “As long as the PINN is trained well, it also generalizes well”*



Rahaman et al., *On the spectral bias of neural networks*, ICML (2019)

# Finite Basis Physics-Informed Neural Networks (FBPINNs)

In the **finite basis physics informed neural network (FBPINNs) method** introduced in **Moseley, Markham, and Nissen-Meyer (2023)**, we employ the **PINN** approach and **hard enforcement of the boundary conditions**; cf. **Lagaris et al. (1998)**.

FBPINNs use the **network architecture**

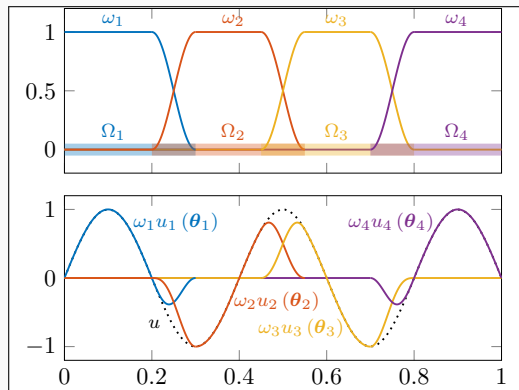
$$u(\theta_1, \dots, \theta_J) = \mathcal{C} \sum_{j=1}^J \omega_j u_j(\theta_j)$$

and the **loss function**

$$\mathcal{L}(\theta_1, \dots, \theta_J) = \frac{1}{N} \sum_{i=1}^N \left( n \left[ \mathcal{C} \sum_{x_i \in \Omega_j} \omega_j u_j \right] (x_i, \theta_j) - f(x_i) \right)^2.$$

Here:

- **Overlapping DD:**  $\Omega = \bigcup_{j=1}^J \Omega_j$
- **Partition of unity**  $\omega_j$  with  $\text{supp}(\omega_j) \subset \Omega_j$  and  $\sum_{j=1}^J \omega_j \equiv 1$  on  $\Omega$



## Hard enf. of boundary conditions

Loss function

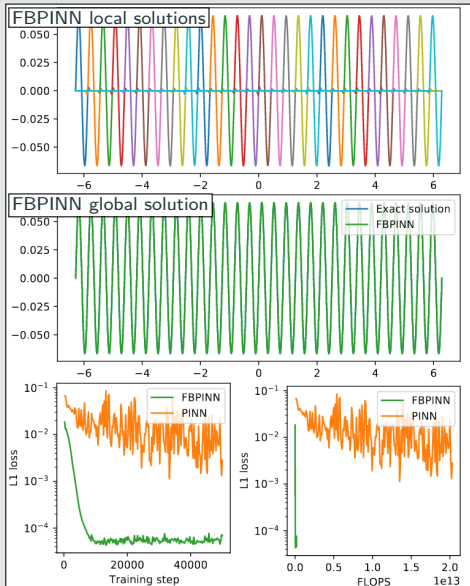
$$\mathcal{L}(\theta) = \frac{1}{N} \sum_{i=1}^N \left( n \left[ \mathcal{C} u \right] (x_i, \theta) - f(x_i) \right)^2,$$

with constraining operator  $\mathcal{C}$ , which **explicitly enforces the boundary conditions**.



# Numerical Results for FBPINNs

## PINN vs FBPINN (Moseley et al. (2023))



## Scalability of FBPINNs

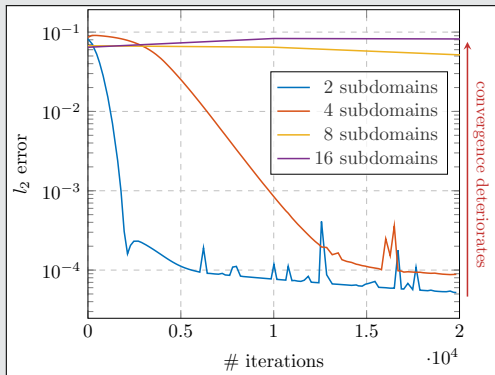
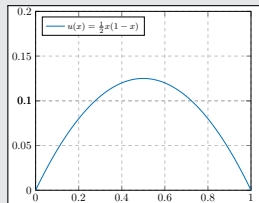
Consider the **simple** boundary value problem

$$-u'' = 1 \text{ in } [0, 1],$$

$$u(0) = u(1) = 0,$$

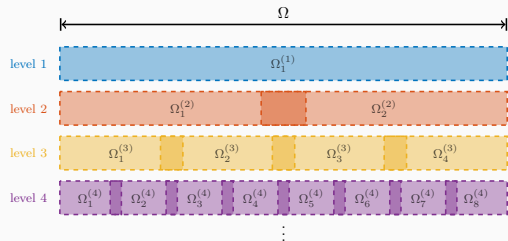
which has the **solution**

$$u(x) = 1/2x(1 - x).$$



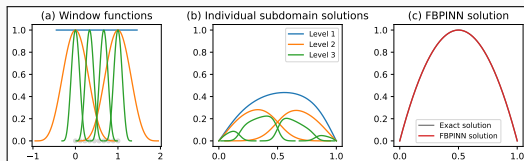
# Multi-Level FBPINN Algorithm

Extension of FBPINNs to  $L$  levels; Cf. **Dolean, Heinlein, Mishra, Moseley (2024)**.



## $L$ -level network architecture

$$u(\theta_1^{(1)}, \dots, \theta_{J^{(L)}}^{(L)}) = e \left( \sum_{l=1}^L \sum_{i=1}^{N^{(l)}} \omega_j^{(l)} u_j^{(l)}(\theta_j^{(l)}) \right)$$



## Multi-Frequency Problem

Let us now consider the two-dimensional multi-frequency Laplace boundary value problem

$$-\Delta u = 2 \sum_{i=1}^n (\omega_i \pi)^2 \sin(\omega_i \pi x) \sin(\omega_i \pi y) \quad \text{in } \Omega,$$

$$u = 0 \quad \text{on } \partial\Omega,$$

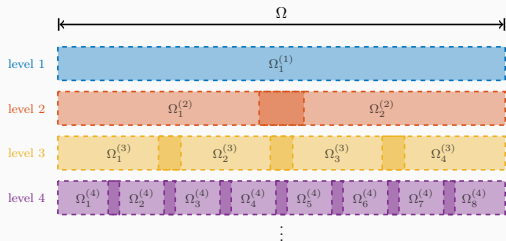
with  $\omega_i = 2^i$ .

For increasing values of  $n$ , we obtain the analytical solutions:



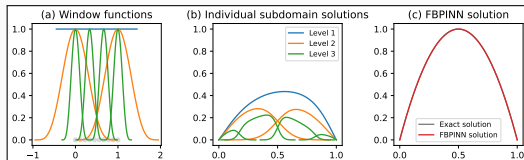
# Multi-Level FBPINN Algorithm

Extension of FBPINNs to  $L$  levels; Cf. [Dolean, Heinlein, Mishra, Moseley \(2024\)](#).



## $L$ -level network architecture

$$u(\theta_1^{(1)}, \dots, \theta_{J^{(L)}}^{(L)}) = e \left( \sum_{l=1}^L \sum_{i=1}^{N^{(l)}} \omega_j^{(l)} u_j^{(l)}(\theta_j^{(l)}) \right)$$



## Multi-Frequency Problem

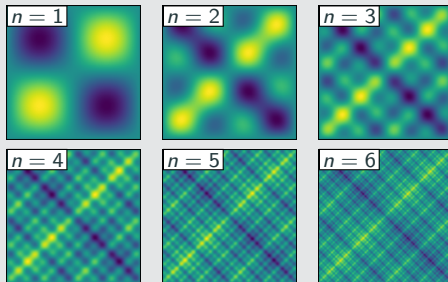
Let us now consider the **two-dimensional multi-frequency Laplace boundary value problem**

$$-\Delta u = 2 \sum_{i=1}^n (\omega_i \pi)^2 \sin(\omega_i \pi x) \sin(\omega_i \pi y) \quad \text{in } \Omega,$$

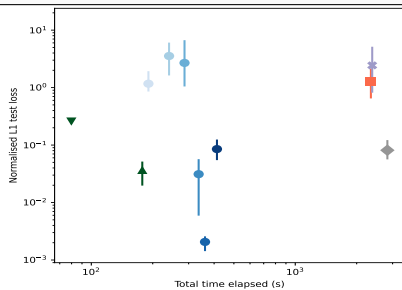
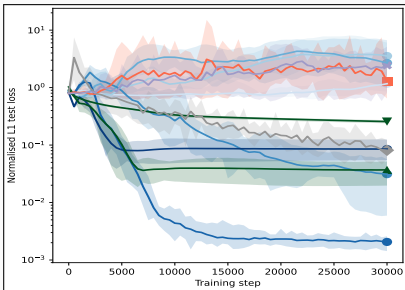
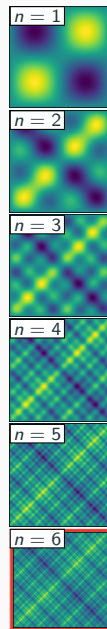
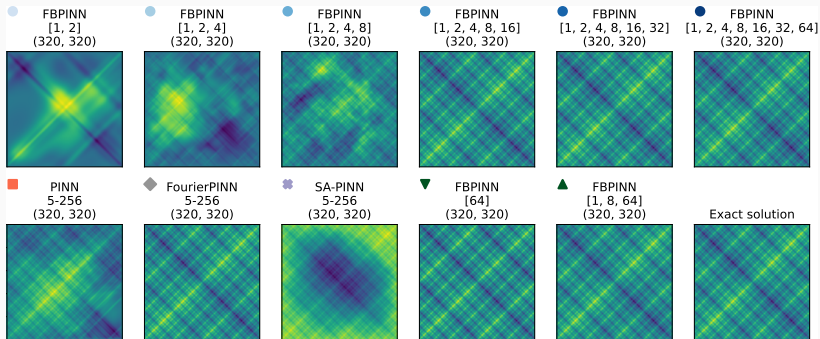
$$u = 0 \quad \text{on } \partial\Omega,$$

with  $\omega_i = 2^i$ .

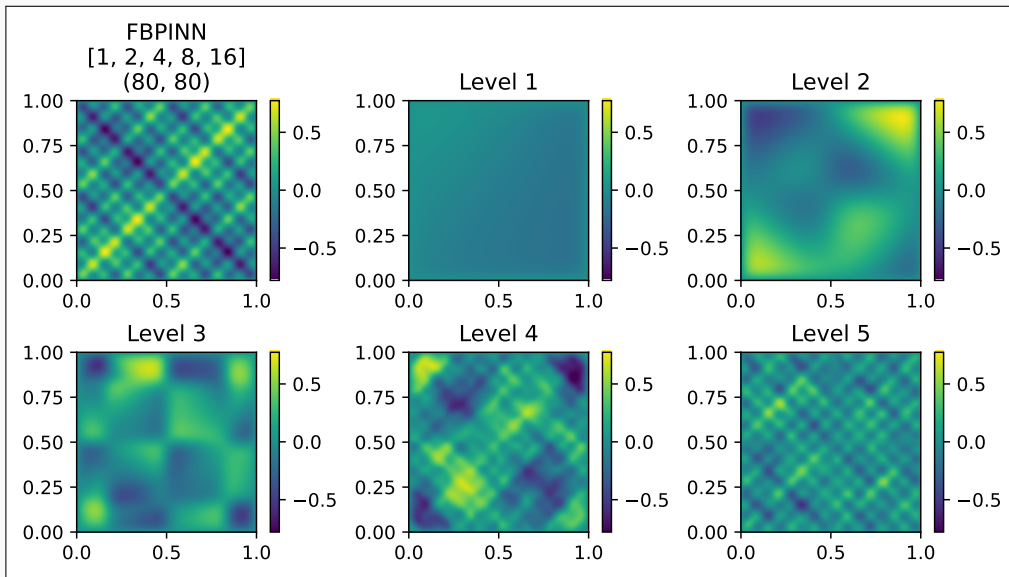
For increasing values of  $n$ , we obtain the **analytical solutions**:



# Multi-Level FBPINNs for a Multi-Frequency Problem – Strong Scaling

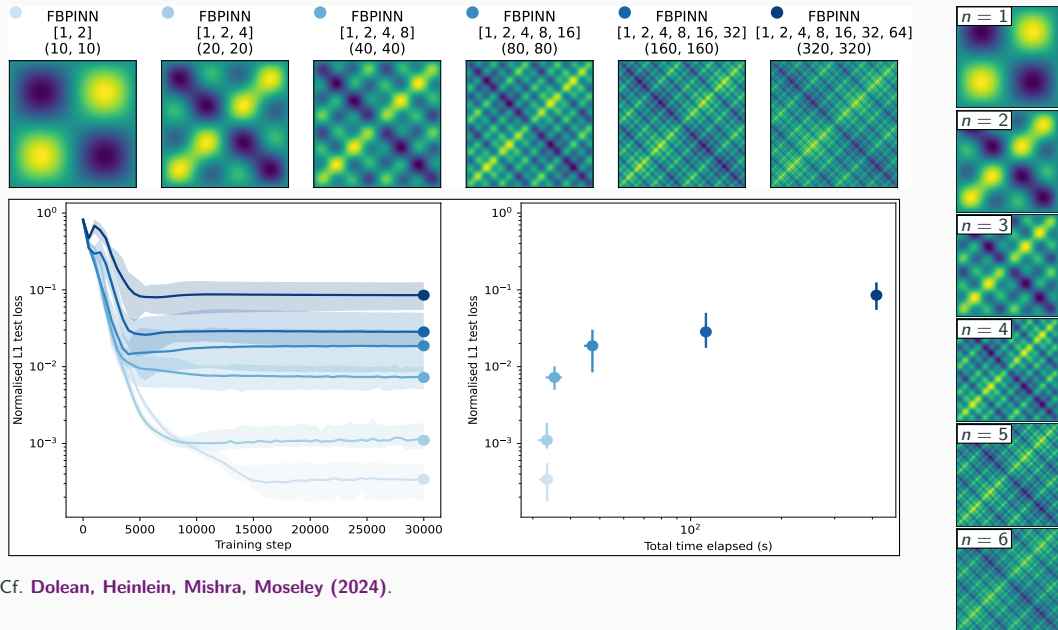


# Multi-Frequency Problem – What the FBPINN Learns

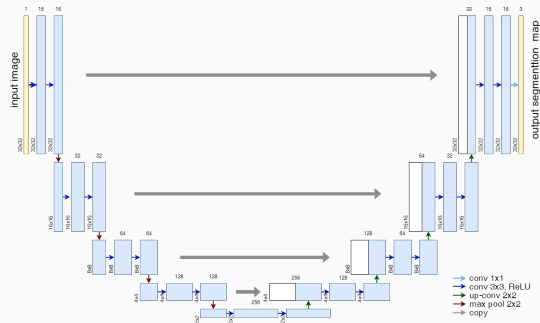


Cf. [Dolean, Heinlein, Mishra, Moseley \(2024\)](#).

# Multi-Level FBPINNs for a Multi-Frequency Problem – Weak Scaling



# Memory Requirements for CNN Training

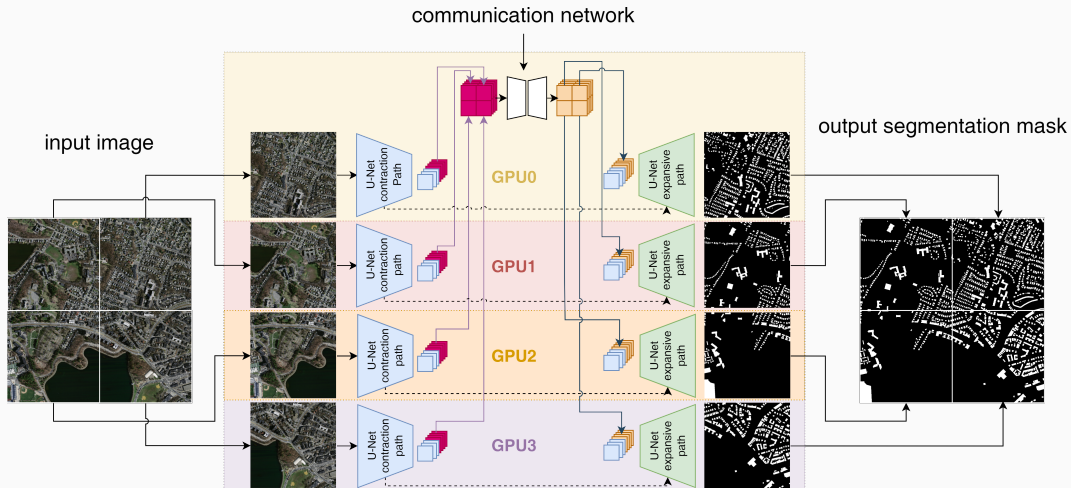


- As an example for a **convolutional neural network (CNN)**, we employ the **U-Net architecture** introduced in **Ronneberger, Fischer, and Brox (2015)**.
- The U-Net yields **state-of-the-art accuracy** in **semantic image segmentation** and other **image-to-image tasks**.

*Below: memory consumption for training on a single  $1024 \times 1024$  image.*

name	size	# channels		mem. feature maps		mem. weights	
		input	output	# of values	MB	# of values	MB
input block	1 024	3	64	268 M	<b>1 024.0</b>	38 848	<b>0.148</b>
encoder block 1	512	64	128	167 M	<b>704.0</b>	221 696	<b>0.846</b>
encoder block 2	256	128	256	84 M	<b>352.0</b>	885 760	<b>3.379</b>
encoder block 3	128	256	512	42 M	<b>176.0</b>	3 540 992	<b>13.508</b>
encoder block 4	64	512	1 024	21 M	<b>88.0</b>	14 159 872	<b>54.016</b>
decoder block 1	64	1,024	512	50 M	<b>192.0</b>	9 177 088	<b>35.008</b>
decoder block 2	128	512	256	101 M	<b>384.0</b>	2 294 784	<b>8.754</b>
decoder block 3	256	256	128	201 M	<b>768.0</b>	573 952	<b>2.189</b>
decoder block 4	512	128	64	402 M	<b>1 536.0</b>	143 616	<b>0.548</b>
output block	1 024	64	3	3.1 M	<b>12.0</b>	195	<b>0.001</b>

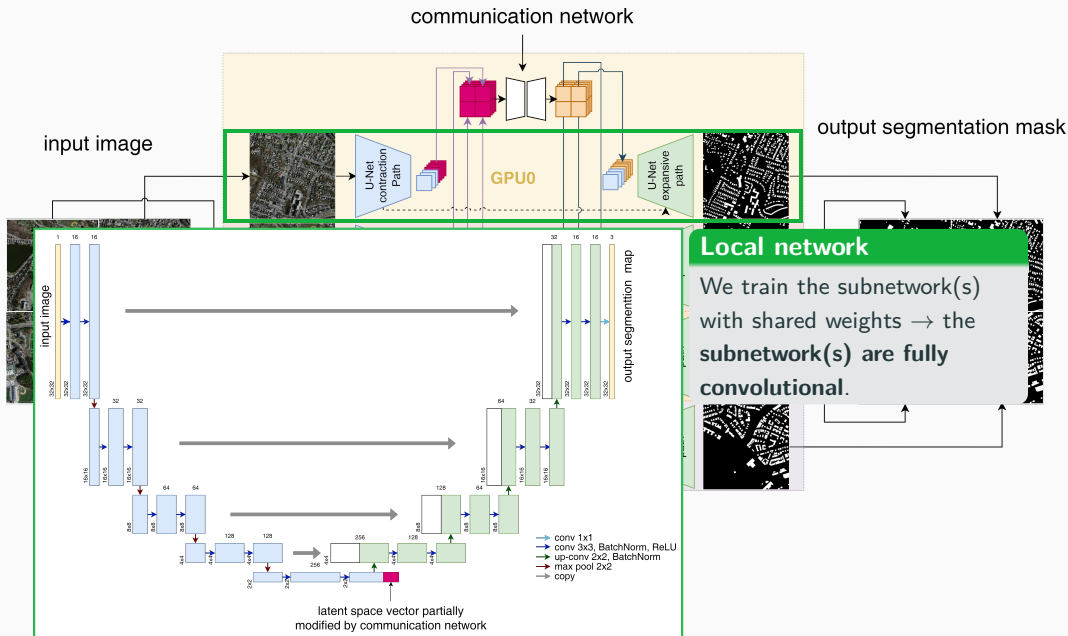
# Decomposing the U-Net



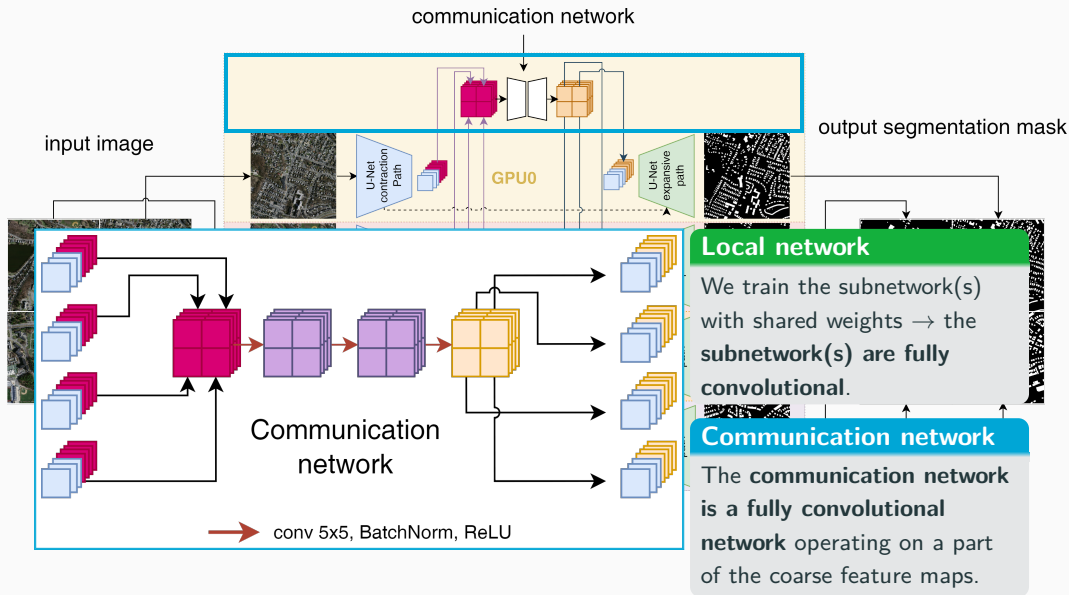
Cf. [Verburg, Heinlein, Cyr \(subm. 2024\)](#).



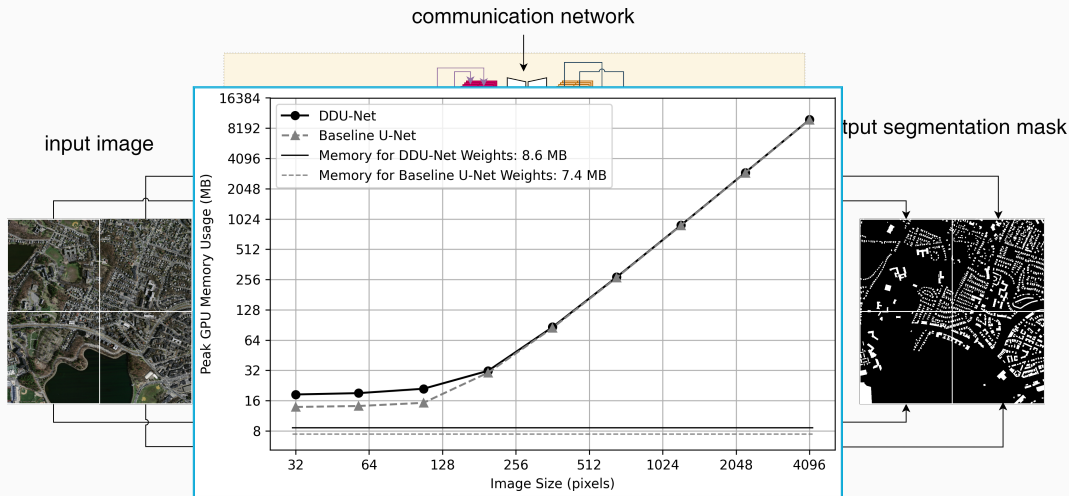
# Decomposing the U-Net



# Decomposing the U-Net



# Decomposing the U-Net

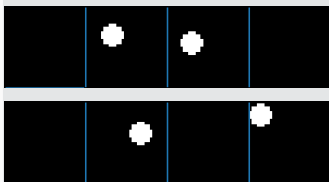


- Distribution of feature maps results in **significant reduction of memory usage on a single GPU**
- **Moderate additional memory usage** due to the **communication network**

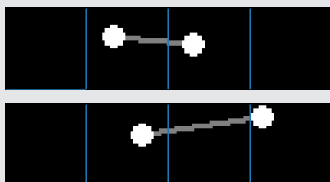
# Results – Synthetic Data Set

Task: Connect two dots via a line segment

Input

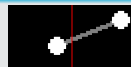


Target (segmentation mask)



Result: Communication

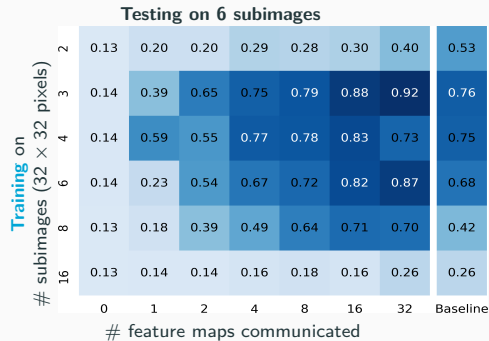
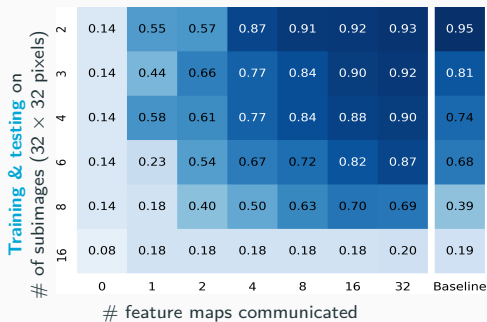
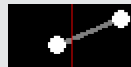
True mask



Pred. (no comm.)



Pred. (comm.)



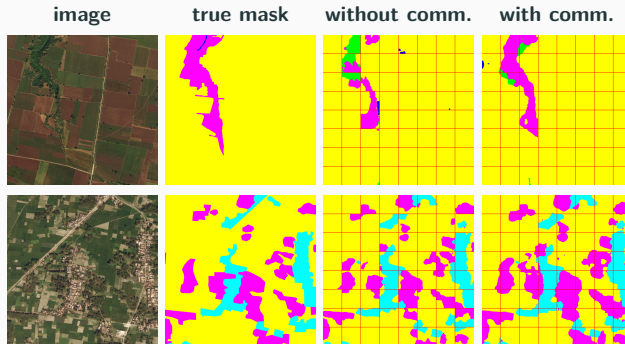
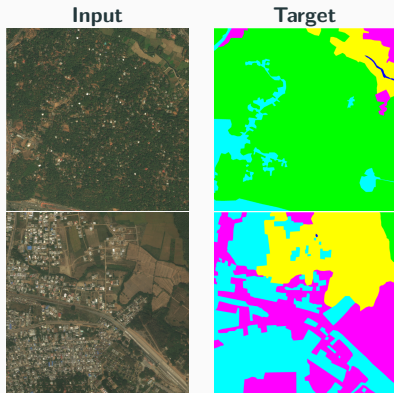
# DeepGlobe 2018 Satellite Image Data Set (Demir et al. (2018))

class	pixel count	proportion
urban	642.4M	9.35 %
agriculture	3898.0M	56.76 %
rangeland	701.1M	10.21 %
forest	944.4M	13.75 %
water	256.9M	3.74 %
barren	421.8M	6.14 %
unknown	3.0M	0.04 %

## Avoiding overfitting

The data set includes **only 803 images**. To **avoid overfitting**, we

- apply **batch normalization**, use **random dropout** layers and **data augmentation**, and
- **initialize the encoder** using the **ResNet-18** (He, Zhang, Ren, and Sun (2016))



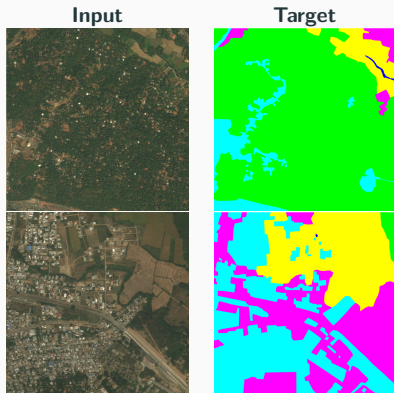
# DeepGlobe 2018 Satellite Image Data Set (Demir et al. (2018))

class	pixel count	proportion
urban	642.4M	9.35 %
agriculture	3898.0M	56.76 %
rangeland	701.1M	10.21 %
forest	944.4M	13.75 %
water	256.9M	3.74 %
barren	421.8M	6.14 %
unknown	3.0M	0.04 %

## Avoiding overfitting


The data set includes **only 803 images**. To **avoid overfitting**, we

- apply **batch normalization**, use **random dropout** layers and **data augmentation**, and
- **initialize the encoder** using the **ResNet-18** (He, Zhang, Ren, and Sun (2016))



## Schwarz Domain Decomposition Preconditioners

- **Numerical scalability** and **robust convergence** for
  - heterogeneous problems
  - multiphysics problems
  - highly nonlinear problems

→ **Algebraic** and **parallel** implementation in FROSch 

## Domain Decomposition for Neural Networks

- Schwarz domain decomposition architectures **improve the scalability of PINNs** to large domains / high frequencies, **keeping the complexity of the local networks low**.
- Novel DDU-Net approach **decouples the training on the sub-images**, allowing us to **distribute the memory load** among multiple GPUs. It **limits communication** to deepest level of the U-Net architecture using a **communication network**.

# Thank you for your attention!